Particulate Matter Variability in Kathmandu based on In-Situ Measurements, Remote Sensing, and Reanalysis Data

Stefan Becker[a], Ramesh Prasad Sapkota[b], Binod Pokharel[c], Loknath Adhikari[d], Rudra Prasad Pokhrel[e], Sujan Khanal[f], and Basant Giri[f]

[a] Ramapo College of New Jersey and City University of New York, Graduate Center, USA
[b] Central Department of Environmental Science, Tribhuvan University, Nepal
[c] Department of Plants, Soils, and Climate, Utah Climate Center, Utah State University, Logan, Utah, USA
[d] Earth System Science Interdisciplinary Center, University of Maryland, USA
[e] Department of Physics, North Carolina A & T State University, USA
[f] Center for Analytical Sciences, Kathmandu Institute of Applied Sciences, Kathmandu, Nepal

Abstract

Kathmandu has one of the highest particulate matter air pollution levels in the world. However, few direct measurement data are available for long-term analyses, limiting policy interventions and public health advisories. Remote sensing based data sets provide an alternative approach. In this paper, we present an approach to analyze and understand the diurnal, seasonal, annual, and multi-annual variability of pollution levels based on in situ measurements of $PM_{2.5}$, remote sensing data based on Moderate Resolution Imaging Spectroradiometer (MODIS) Aqua and Terra Aerosol Optical Depth (AOD), and $PM_{2.5}$ data, as well as from Copernicus Atmosphere Monitoring Service (CAMS) and Modern-Era Retrospective Analysis for Research and Applications, Version 2 (MERRA-2) reanalysis data sets. The analysis of the direct measurements revealed distinct annual patterns, characterized by winter maxima and summer minima. With the exception of the summer monsoon season, public health guidelines are frequently exceeded significantly throughout the year, particularly in winter. The analysis furthermore pointed toward distinct daily patterns with primary maxima in the mornings, secondary maxima in the late evenings, and minima in the afternoons. The annual pattern of AOD derived from the MODIS data is markedly different from that. Due to the coarse spatial resolution and the fact that MODIS AOD is a column integrated property, it does not reflect the small scale phenomenon of the Kathmandu urban pollution pattern but instead shows a maximum in the spring. The same pattern was observed with the CAMS and MERRA-2 reanalysis AOD data, even though MERRA-2 captures pollution levels during the summer monsoon season very well. The CAMS reanalysis $PM_{2.5}$ data are generally well-aligned with the near-surface measurement data, even though they overestimate the daily and monthly maxima and do not capture the

morning maxima in the diurnal course. Nevertheless, CAMS $PM_{2.5}$ data can be adjusted via linear regression to reasonably mirror the measurements. It shows that $PM_{2.5}$ concentrations in Kathmandu have increased significantly in the past decades (almost 2 $\mu g/m^3$ annually), mainly after the monsoon season from September to February. As a result, around 85 percent of all winter days in Kathmandu are categorized as "unhealthy" according to the Air Quality Index (AQI).

Keywords: Air Pollution, PM2.5, Aerosol Optical Depth, CAMS, MERRA, MODIS, Air Quality

1. Introduction

1.1. Air Pollution in the Kathmandu Valley

The complex impact of particulate matter air pollution on climate change has been the topic of numerous studies (e.g., Kaufman et al., 2002; Rosenfeld et al., 2008; Li et al., 2011; IPCC, 2013; Wang et al., 2014a; Guo et al., 2016a) throughout the last decades. The deleterious health effects, ranging from cardiovascular and respiratory diseases to premature deaths has also been well documented (e.g., EPA, 2020, Al-Saadi et al., 2005; Vidot et al., 2007; Wang et al., 2010; Gurung and Bell, 2012; Apte et al., 2015; Schwartz et al., 2015). Understanding the variability of particulate matter air pollution is therefore crucial to developing meaningful reduction strategies (Wang and Christopher, 2003; Lin et al., 2015; Guo et al., 2016b)

Nepal consistently ranks as having one of the worst particulate air pollution levels worldwide. The 2016 Environmental Performance Index (EPI) ranked Nepal 177th out of 180 countries in terms of air pollution (Hsu et al., 2016; Bhattarai, 2020). One of the worst affected areas in Nepal is the Kathmandu Valley, located in the mid-hills of Nepal at a latitude of 27.7°N (Figure 1).

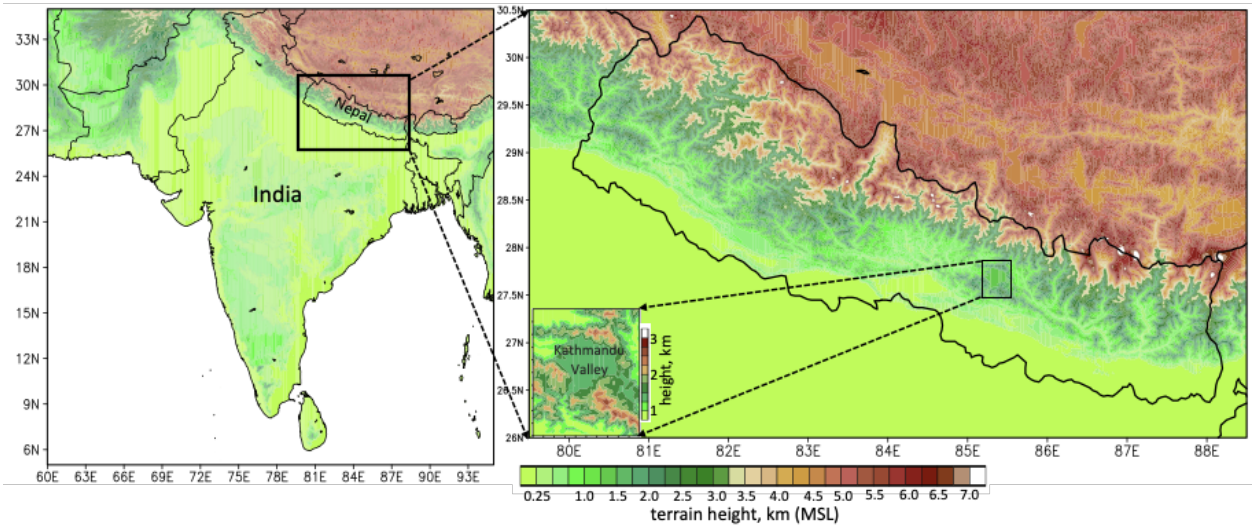

Figure 1: Topographic map of South Asia and Nepal

Although many major cities in the developing world face elevated air pollution levels, Kathmandu is especially vulnerable due to multiple reasons:

A) Topography: The valley is shaped like a circular bowl at approximately 1300 m above sea level, which is surrounded by a ring of mountains ranging from 2000 to 2800 m above sea level (Panday et al. 2009). This particular topography restricts air movement, and pollutants generated in the valley are often trapped within the valley (Clean Energy Nepal, 2003).

B) Atmospheric conditions: Particularly during the winters, strong nighttime temperature inversions trap the air pollution near the ground. This effect is compounded by the fact that the vast majority of Kathmandu's rainfall occurs during the monsoon season in summer while the rest of the year is relatively dry, and, particularly in winter, the pollutants are unlikely to be washed out by precipitation.

C) Increase in population, traffic, and industrial activity: Rapid urban growth, dense settlements with minimal open space, refuse burning, polluting industries operating under inadequate environmental standards, a poor road network with often unpaved and congested roads, poor quality vehicles and fuels combined with lacking emission inspections and maintenance, and a poorly managed transportation system all contribute to a tremendous output of particulate air pollution. For example, Faiz et al. (2006) and Shrestha et al. (2013) found that between 1990 and 2014, the total vehicle fleet grew from less than 50,000 to more than 700,000, with the number of motorcycles having the highest annual growth rate of 16% during the period. Mool et al. (2020) identified the lack of routine vehicle maintenance as one of the aggravating factors.

D) Crop residue burning from agriculture in northern India and Nepal contribute significantly to particulate matter pollution levels in Nepal. Pollutants are transported into the Kathmandu Valley (Mahapatra et al., 2019),
E) Additional particulate matter air pollution stems from the open burning of municipal solid waste (Saikawa et al. 2020) and domestic biofuel usage (Zhong et al., 2019).

1.2. Previous studies

Sharma (1997) pointed to Kathmandu's energy consumption and heavy air pollution, particularly in winter months, when a thick layer of fog covers the valley up to 10 AM. Early monitoring and documentation of air pollution in the Kathmandu Valley was done in the 1990s by several organizations funded by the World Bank (ICIMOD, 2007). The study identified particulate matter as the primary pollutant of concern and vehicles as the main pollution source.

One of the first comprehensive monitoring campaigns on particulate air pollutants in the Kathmandu Valley was done from 2003 to 2005 by the Ministry of Population and Environment (MOPE) with support from the Danish International Development Agency (DANIDA). The annual averages of PM_{10} levels were found to be 6-7 times higher than the WHO guideline of 20 μg m^{-3}. Giri et al. (2006) found particulate PM_{10} concentrations measured at roadside areas to be persistently higher than at the background sites. Panday and Prinn (2009), based on measurements during the dry season of 2004–2005, noted a very regular pattern of morning and evening peaks in PM_{10} occurring daily in the valley bottom, interspersed with low values in the afternoons and at night. Panday et al. (2009) simulated Kathmandu Valley's meteorology with a mesoscale meteorological model to understand airflows that affect pollution levels.

Another study in 2014, conducted by the Nepal Health Research Council (NHRC), found that annual average $PM_{2.5}$ levels were approximately five times higher than the WHO guideline of 10 μg m^{-3} (Srijan Lal, 2018). The study also revealed distinct annual and daily variability: Particulate pollution levels were almost four times higher (70-80 μg m^{-3}) in the dry seasons compared to the wet seasons. The average daily curve was characterized by a primary peak in the morning and a secondary peak in the late evening (Srijan Lal, 2018). Gurung and Bell (2012) investigated personal exposure to $PM_{2.5}$ and found extremely high values (hourly maximum > 500 μg m^{-3}) for traffic police officers in Kathmandu during morning rush hours (8 AM -11 AM).

Based on measurements at an urban location of Kathmandu Valley from May 2009 to April 2010, Sharma et al. (2012) concluded that the lowest concentration of black carbon was found during the monsoon and post-monsoon seasons. Analyzing diurnal variations, they found peaks around 9 AM and 8 PM local time and minima typically occurring in the

afternoons. Based on the data recorded and modeled in the SusKat-ABC international air pollution measurement campaign (2012-2013), Putero et al. (2015) investigated aerosol levels at Paknajol in the city center of Kathmandu. They concluded that the diurnal behavior of black carbon and aerosol number concentration is mainly dependent on local pollution sources.

Shakya et al. (2017) measured hourly average $PM_{2.5}$ concentrations in the vicinity of six major road intersections in the Kathmandu Valley and observed levels up to almost 800 μg m^{-3} with 5 min maxima reaching above 1000 μg m^{-3} during spring 2014. Islam et al. (2015) analyzed pre-monsoon air pollution levels in the Kathmandu Valley as part of the Nepal Ambient Monitoring and Source Testing Experiment (NAMaSTE) and found daily average $PM_{2.5}$ concentrations ranging between 30 to 207 μg m^{-3} during a 2-week measurement campaign in April 2015. Mues et al. (2018) simulated the meteorology and black carbon concentrations in the Kathmandu Valley based on the Weather Research and Forecast (WRF) model. A recent study reported cancer causing asbestos materials in the dust collected from core areas of Kathmandu (Neupane et al., 2020). Sadavarte et al. (2019) provide a preliminary approach leading to an emission inventory for Nepal.

1.3. Study goals

There have been numerous studies regarding the air pollution in Kathmandu Valley for short time scales (from months to about years); however, little is known about the annual and decadal pattern of particulate matter pollution in Kathmandu. Part of the reason for this is due to the lack of long-term measurement data.

This study aims to assess and compare diurnal, annual, and multi-annual variability of particulate matter air pollution levels in Kathmandu based on available direct measurements, remote sensing, and reanalysis data of existing data. We have assessed the diurnal and seasonal variability of the recent pollution levels in the city and how they can be categorized in terms of their public health impacts. Given the relatively short period for which direct measurements are available, the assessment of the correlation between the data sets will allow for conclusions on how the pollution levels have changed over the last decades.

2. Data and Methods

2.1. Direct near-surface observations

We obtained the in-situ measurement of hourly average $PM_{2.5}$ data from AirNow, a partnership of various agencies (within and outside the U.S.) with a centralized data system (www.airnow.gov). AirNow provides quality-controlled air pollution data in Kathmandu for two locations: Phora Durbar and the U.S. Embassy. Given that both sites' data are fairly

similar, we only used the data of one station, Phora Durbar, for further analyses. The station is located in central Kathmandu. Hourly data of $PM_{2.5}$ concentrations are available since February 2017. We calculated means and standard deviation for hourly, daily, and monthly values and subcategorized the results based on the season (winter (December-February), pre-monsoon (March-May), summer monsoon (June-August), post-monsoon (September-November). It is debatable whether September should instead be included in the monsoon season as has been done in some studies; however, this differentiation would not affect the outcomes of this study in a significant way. We evaluated the daily observed $PM_{2.5}$ levels based on the NAAQS (National Ambient Air Quality Standards) published by the United States Environmental Protection Agency (EPA, 2016), according to which the 24-hour primary and secondary PM2.5 standard is 35 μg m^{-3}. The annual average primary EPA standard is 12 μg m^{-3}; the corresponding WHO guideline value is 10 μg m^{-3}. We furthermore classified the observed near ground PM pollution levels according to the Air Quality Index (Table 1, EPA, 2012).

AQI Category	AQI Value	24-hour $PM_{2.5}$ concentration (μg m^{-3})
Good	0 - 50	0 - 15.4
Moderate	51 - 100	15.5 - 40.4
Unhealthy for sensitive groups	101 - 150	40.5 - 65.4
Unhealthy	151 - 200	65.5 - 150.4
Very unhealthy	201 - 300	150.5 - 250.4
Hazardous	> 300	> 250.5

Table 1: EPA - Air Quality Index (AQI) for $PM_{2.5}$

2.2. Satellite Data

A combination of satellite remote sensing and ground-based observations has been increasingly used to assess pollution variability at various scales (Fylonchyk et al., 2019). However, Guo et al. (2017) pointed toward the difficulty to derive accurate $PM_{2.5}$ data through satellite observations due to the elusive relationship between $PM_{2.5}$ and aerosol optical depth (AOD), which is further complicated by meteorological factors. Just et al. (2018) utilized machine learning methods to correct errors based on AOD data in the Northeastern USA.

Moderate Resolution Imaging Spectroradiometer (MODIS), a key instrument in the NASA satellites Terra and Aqua, measures emitted and reflected radiances in 36 spectral bands across visible and infrared spectra extending from 0.415 to 14.235 μm with variable nadir resolution of 250, 500, and 1000 m. It was launched aboard the Terra satellite in December 1999, and later aboard the Aqua satellite in May 2002. It is well-suited to measure cloud and aerosol properties (King et al. 1992). Both MODIS instruments are currently operational and providing radiance measurements.

MODIS aerosol product monitors aerosol types, optical thickness, mass concentration, and particle size distribution at 10 km x 10 km horizontal resolution at nadir (Tanré et al. 1996, Levy et al. 2013). The broad range of spectral bands of MODIS allows measurements at these different bands. During clear sky conditions, the radiance signature of aerosols is different from the background molecules, which enables retrieval of aerosol properties using radiances in various spectral bands (Remer et al. 2005). The 10 km x 10 km resolution is used for the aerosol retrieval instead of the much finer native resolution of the radiance measurements because of the need to increase the signal to noise ratio (Tanré et al. 1996).

In this study, MODIS Level 2 aerosol optical depth (AOD) and aerosol (column integrated) concentration data from 2015 to 2019 are used. The Terra and Aqua satellites overpass the Kathmandu Valley almost daily at around 10 AM and 1:30 PM local time, respectively, allowing daily AOD and concentration data, one in the morning and another in the afternoon. Aerosol data are not available during overcast conditions. This results in the availability of very few daily measurements during the summer monsoon season.

The aerosol data over the Kathmandu Valley are derived from the closest 10 x 10 km MODIS aerosol pixel. If the data are not available at the nearest pixel, the average of 3x3 and 5x5 aerosol pixels is taken into consideration and averaged to represent the aerosol concentration over Kathmandu. The monthly averages are calculated using available daily values for each month in the five years from Jan 2015 through Dec 2019.

2.3. Reanalysis Data

In addition to in-situ measurements of PM2.5 and the MODIS data, we utilized reanalysis data to investigate how the coarser-resolution gridded data capture the pollution over South Asia and particularly in Kathmandu, Nepal. For that purpose, we used two reanalysis data sets: CAMS and MERRA-2.

The Copernicus Atmosphere Monitoring Service (CAMS, Inness et al., 2019) atmospheric composition (A.C.) dataset is produced by the European Center for Medium-Range Forecasting (ECMWF, Fleming et al., 2017; Inness et al., 2015). CAMS reanalysis data

capture several aerosols and pollutants in four-dimensions with a spatial resolution of $0.7^{o} \times 0.7^{o}$. CAMS data are available from 2003 to 2019 at a three-hour temporal resolution. Since observational data are collected only for a limited period in Kathmandu (only three years), they cannot be utilized meaningfully for trend analyses. The reanalysis data can informational gap if they are well-aligned with the observational data.
For comparison with the surface observations, we analyzed monthly $PM_{2.5}$ levels from CAMS. To our best knowledge, CAMS $PM_{2.5}$ data have not been validated with near-surface observations in the region. Therefore, we aim at investigating how the seasonal and diurnal pollution variations based on the CAMS data compare to the near ground observations and whether CAMS data can indeed be used with confidence to examine pollution trends.
We extended our analyses from Nepal to the South Asia region because the highly polluted Indo Gangetic Plain is a major source for the transboundary pollution transport to Nepal. The estimation of air pollution levels in Kathmandu is based on the nearest grid point.

The Modern-Era Retrospective Analysis for Research and Applications, Version 2 (MERRA-2), is the updated version of the National Aeronautics and Space Administration (NASA) latest reanalysis for the satellite era MERRA-1. MERRA-2 is based on the Goddard Earth Observing System, version 5 (GEOS-5), Earth system model, and uses three-dimensional variational data assimilation Gridpoint Statistical Interpolation analysis system (GSI, Buchard et al., 2017; Randles et al., 2017). GEOS-5 is radiatively coupled to the Goddard Chemistry Aerosol Radiation and Transport model (GOCART) aerosol model, which simulates five different types of particulate matters, namely black carbon (B.C.), organic carbon (O.C.), dust, sea salt, and sulfate. Aerosol optical properties on GOCART are primarily based on the Optical Properties of Aerosol and Clouds (OPAC) database (Buchard et al., 2017; Randles et al., 2017). MERRA-2 incorporates the bias-corrected AOD from the MODIS Terra and Aqua satellites as well as from the space-based Advanced Very High-Resolution Radiometer (AVHRR) over the ocean. In addition, non-bias-corrected AOD is also incorporated from Multi-Angle Imaging SpectroRadiometer (MISR) over bright surfaces and from ground-based Aerosol Robotic Network (AERONET) stations. More details about the product validation, system evaluation, emission inventories, and aerosol assimilation system can be found in the MERRA-2 evaluation and system descriptions papers (Buchard et al., 2017; Randles et al., 2017). The model resolution is $0.583^{o} \times 0.6258^{o}$ latitude by longitude with 72 hybrid-eta layers from the surface to 0.01 hPa.

The surface concentrations of $PM_{2.5}$ reported by the MERRA-2 are calculated from five parameters as

$$PM_{2.5} = BC + 1.6 * OC + Dust_{2.5} + Sea\ Salt_{2.5} + 1.375 * SO_4$$

where BC, OC, $Dust_{2.5}$, Sea $Salt_{2.5}$, and SO_4 are the concentration of black carbon, organic carbon, dust, sea salt, and sulfate ions with a diameter of less than 2.5 μm. Since the

GOCART model does not report the nitrate aerosol in the model, this could underestimate the concentration compared to ground-based measurements. Like CAMS, the estimated values are based on the nearest grid point of the Kathmandu location.

3. Results and Interpretation

3.1. Direct near-surface measurements

The $PM_{2.5}$ levels at Phora Durbar followed a distinct annual cycle with a winter maximum, a summer minimum, and regular transitions in between (Figure 2). In the winter months, the average values are around 100 µg m^{-3}; however, the standard deviation points toward a considerable variance of the data. In the summer months, the average values are less than 30 µg m^{-3} with minima in July and August around 17 µg m^{-3}. We observed a continuous increase in average pollution levels from the summer minimum to the maximum in January (105 µg m^{-3}) and a subsequent decrease toward the summer months.

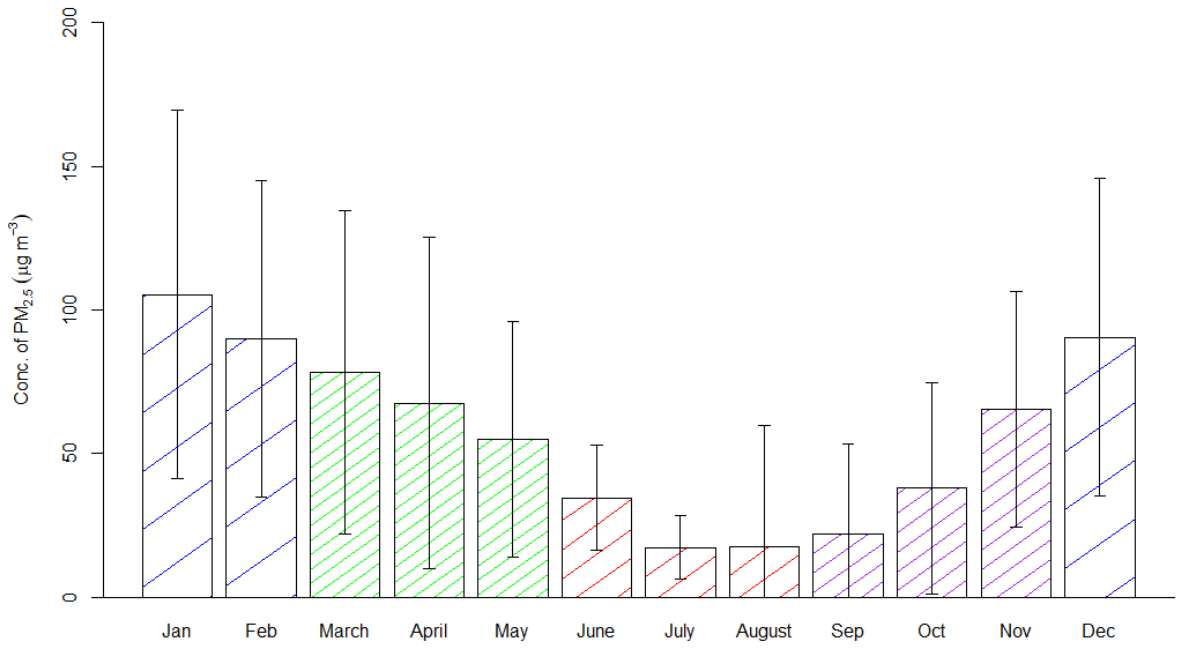

Figure 2: Monthly averages and standard deviations of $PM_{2.5}$ levels measured at Phora Durbar. The column hatches symbolize the seasons.

Based on the assumption that local polluting factors such as high-volume traffic and industrial activities do not vary considerably throughout the year, the observed variability has to be the result of atmospheric conditions and/or long-range transportation patterns. Given the location in the Kathmandu Valley, it is reasonable to conclude that the prevalence

of lower atmospheric inversion layers, as well as washout effects through precipitation, must have a substantial impact on the near-ground pollution levels. High precipitation associated with the summer monsoon combined with strong convection resulting from high temperatures is likely associated with the relatively low pollution levels. The dry winter season with low temperatures and intense and persistent lower atmospheric inversion layers is likely to result in very high pollution levels.

The hourly average $PM_{2.5}$ data also followed similar trends (Figure 3). The differences between the seasons are also clearly visible with decreasing values from winter to pre-monsoon, post-monsoon, and summer monsoon. The diurnal cycle is most pronounced during the high pollution winter season, although it follows a similar pattern in all seasons. The primary maximum occurs in the morning around 8 to 10 AM. Subsequently, the levels decrease toward a minimum in the afternoon from around 2 to 4 PM. In the later afternoon, numbers increase again toward a secondary maximum in the evening around 9 to 10 PM from when onward they decrease toward a secondary minimum in the early morning around 4 to 5 AM.

During the winter season, the primary morning maxima are around 150 μg m^{-3}, the secondary late evening maxima are about 130 μg m^{-3}, while the afternoon minima are about 50 μg m^{-3}. During the pre-monsoon season, the primary morning maxima are around 100 μg m^{-3}, the secondary late evening maxima are approximately 70 μg m^{-3}, while the afternoon minima are about 50 μg m^{-3}. During the summer monsoon season, the morning maxima are less than 40 μg m^{-3}while the minimum occurs around 4 AM at approximately 15 μg m^{-3}. During the post-monsoon season, the primary morning maxima are around 60 μg m^{-3}, the secondary late evening maxima are about 50 μg m^{-3}, while the afternoon minima are approximately 25 μg m^{-3}.

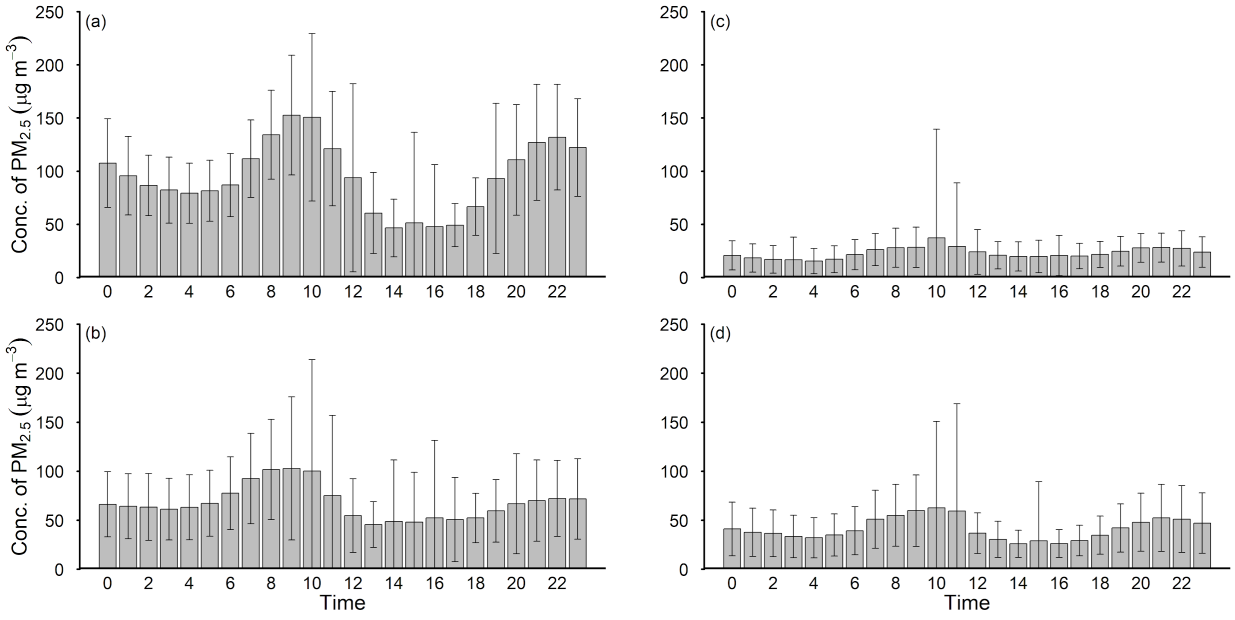

Figure 3: Season-wise hourly variation of $PM_{2.5}$. (a) Winter season, (b) Pre-monsoon, (c) Monsoon, and (d) Post-monsoon

The characteristic diurnal course points toward the pollution levels being strongly determined by local effects. Panday et al. (2009) point toward the results of a mesoscale meteorological model (MM5) to simulate the Kathmandu Valley's meteorology, which explains the dynamics of the basin's nocturnal cold air pool, its dissipation in the morning, and the subsequent growth and decay of the mixed layer over the valley. The primary maximum in the morning is likely associated with the commencement of high-volume traffic and industrial activities. As the inversion layer breaks up due to stronger radiation and surface warming during the late morning, convection and advection cause the pollution levels to decrease in the late morning and the early afternoon. As traffic increases again in the later afternoon and convection is reduced due to decreasing radiation and surface warming toward the evening, pollution levels increase again toward the secondary maximum. Toward midnight and throughout the night, significantly lower traffic and industrial activities result in decreasing pollution. Panday et al. (2009) point toward strong pollution ventilation taking place during the afternoon. The MM5 simulations pointed toward strong westerly winds ventilating the area through the western passes and carrying pollutants through the eastern and southern passes. Panday et al. (2009) further concluded that evening pollutants are lifted by converging katabatic flows before they sink back again toward the surface in the morning.

Despite the substantial variability of daily values (see Figure 2), the pollution levels in winter are so high that the threshold is exceeded on nearly all or all days during these

months at Phora Durbar (Figure 4). Over 80% of the days during the pre-monsoon season exceed the standards. The post-monsoon season is characterized by the highest variability, with exceedances ranging from 2% in September to 94% in November. A sudden drop of exceedances occurs from the pre-monsoon season to the summer monsoon season. While roughly every third day in June is still not meeting the standards, there are only very few or no days in the other summer months for which this is true.

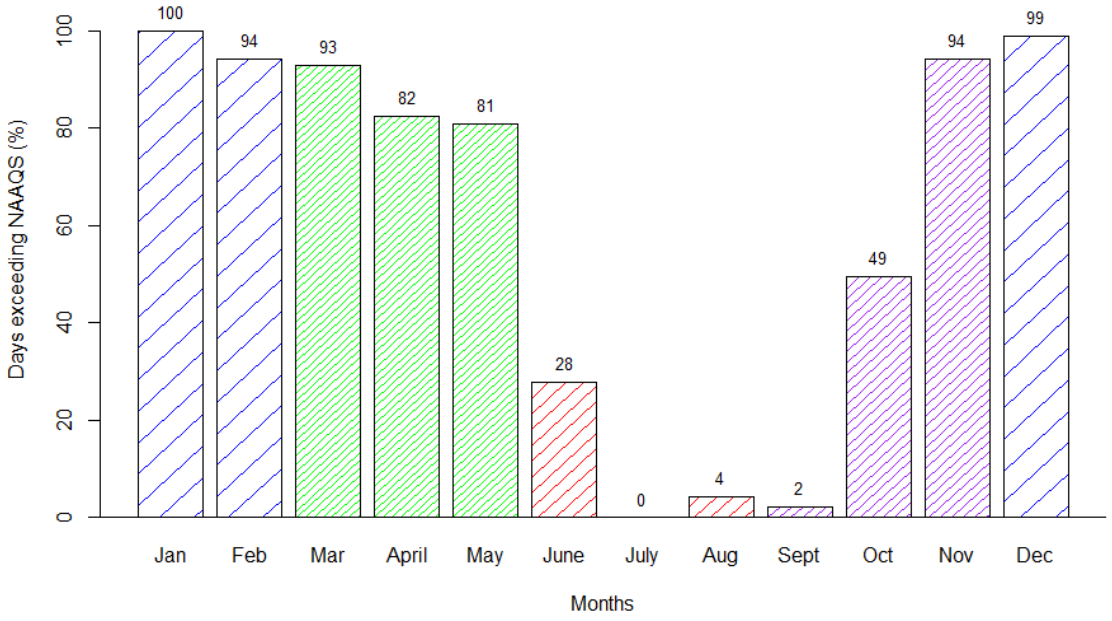

Figure 4: Monthly percentage of days exceeding the NAAQS air quality standards at Phora Durbar.

Figure 5 illustrates the frequency distribution of hourly PM2.5 levels up to 300 µg m^{-3} in intervals of 10 µg m^{-3}. As was to be expected, the distribution has a positive skew. While the highest frequency of cases (over 15%) ranges between 10 and 20 µg m^{-3}, there are significant numbers all across the spectrum. The mean value of almost 60 µg m^{-3} and the median (44 µg m^{-3}) are significantly higher than the EPA or WHO standards. The first and third quartiles of the distribution are 23 µg m^{-3} and 77 µg m^{-3}.

Extreme peak $PM_{2.5}$ pollution levels in Kathmandu are around 300 µg m^{-3}, a level that is almost on the similar order of magnitude of extreme pollution levels found by Dhaka et al. (2020) in April 2020 in the Delhi-National Capital Region (NCR) (300 - 400 µg m^{-3}). It is, however, still considerably lower than the levels Kanawade et al. (2020) documented for stagnant weather conditions in New Delhi in November 2016, during which the AQI exceeded 500, and $PM_{2.5}$ levels significantly exceeded 500 µg m^{-3}.

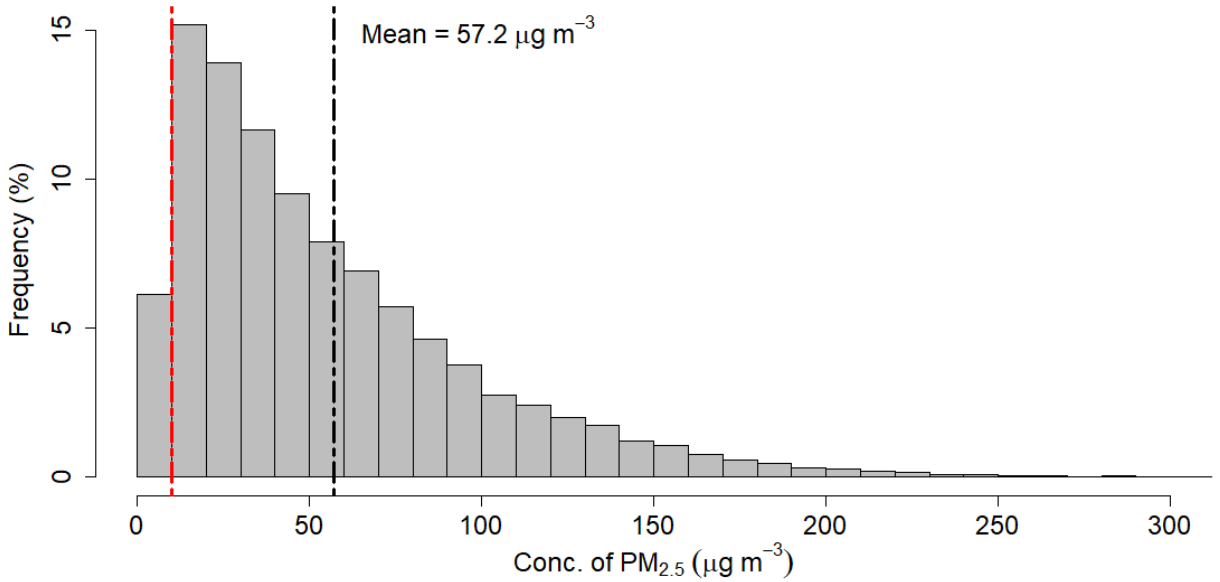

Figure 5: Histogram for the ambient concentration of $PM_{2.5}$. The red line shows the annual WHO Guideline Value (10 μg/m^3 for the annual mean) for $PM_{2.5}$ (Data range from 1 to 985 μg m^{-3})

3.2. MODIS Satellite Data

Figure 8 provides mean seasonal AOD for the pre-monsoon season (March-May) using Aqua MODIS Level 2 data from 2015 to 2020. No data are available for Northern Nepal due to the cloudiness associated with rising air at the Himalaya mountain range. Further, over bright surfaces such as deserts and snow-covered mountain regions, it is difficult to retrieve aerosol properties accurately because the radiance signal is dominated by the surface reflectance. As a result of the spatial resolution of the data, potentially elevated pollution levels in Kathmandu cannot be identified in that image. Elevated AOD values are distinguishable in the highly industrialized Indo-Gangetic Plain in northern India bordering Nepal. Uttar Pradesh, with more than 200 million inhabitants, is the most populous state in India. Major urban industrial centers of the region include New Delhi, Lucknow, and Patna. Elevated pollution levels from that region appear to be spilling over into southern Nepal and are likely to affect Kathmandu to some degree, even though it is not meaningful to assess that quantitatively based on these data. Several studies (e.g., Bonasoni et al. 2010, Ram et al. 2010, Marioni et al., 2011, Putero et al., 2015) have shown that air masses from these highly polluted areas in south Asia can, in fact, move to the Himalayas. Mahapatra et al. (2019) point toward a substantial increase in particulate loading in the Kathmandu Valley and nearby background sites over the past 15 years based on AOD data.

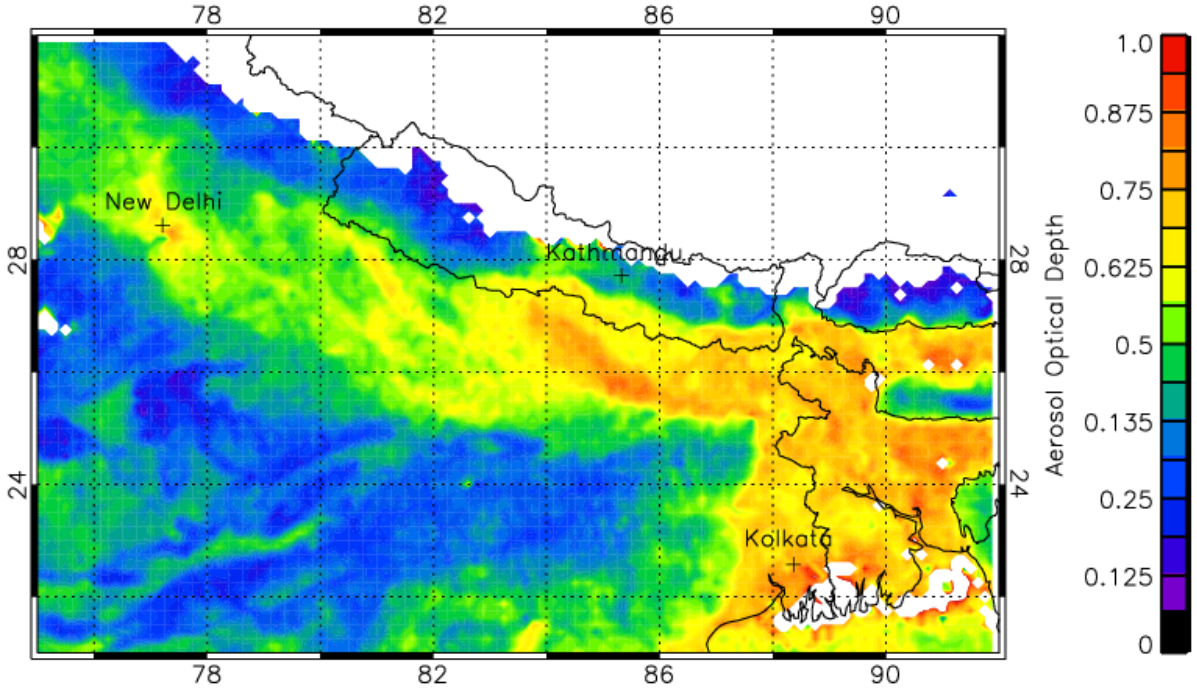

Figure 8: Mean seasonal AOD for the pre-monsoon season (March-May) using Aqua MODIS Level 2 data from 2015 to 2020.

Figure 9 shows the monthly averages and maxima of MODIS data from 2015 to 2019. Both data series are mostly corresponding and are characterized by relatively high values from April to July and relatively low values for the rest of the year. This observation is not well aligned with the conclusion drawn from the near-surface measurements or the CAMS reanalysis data.

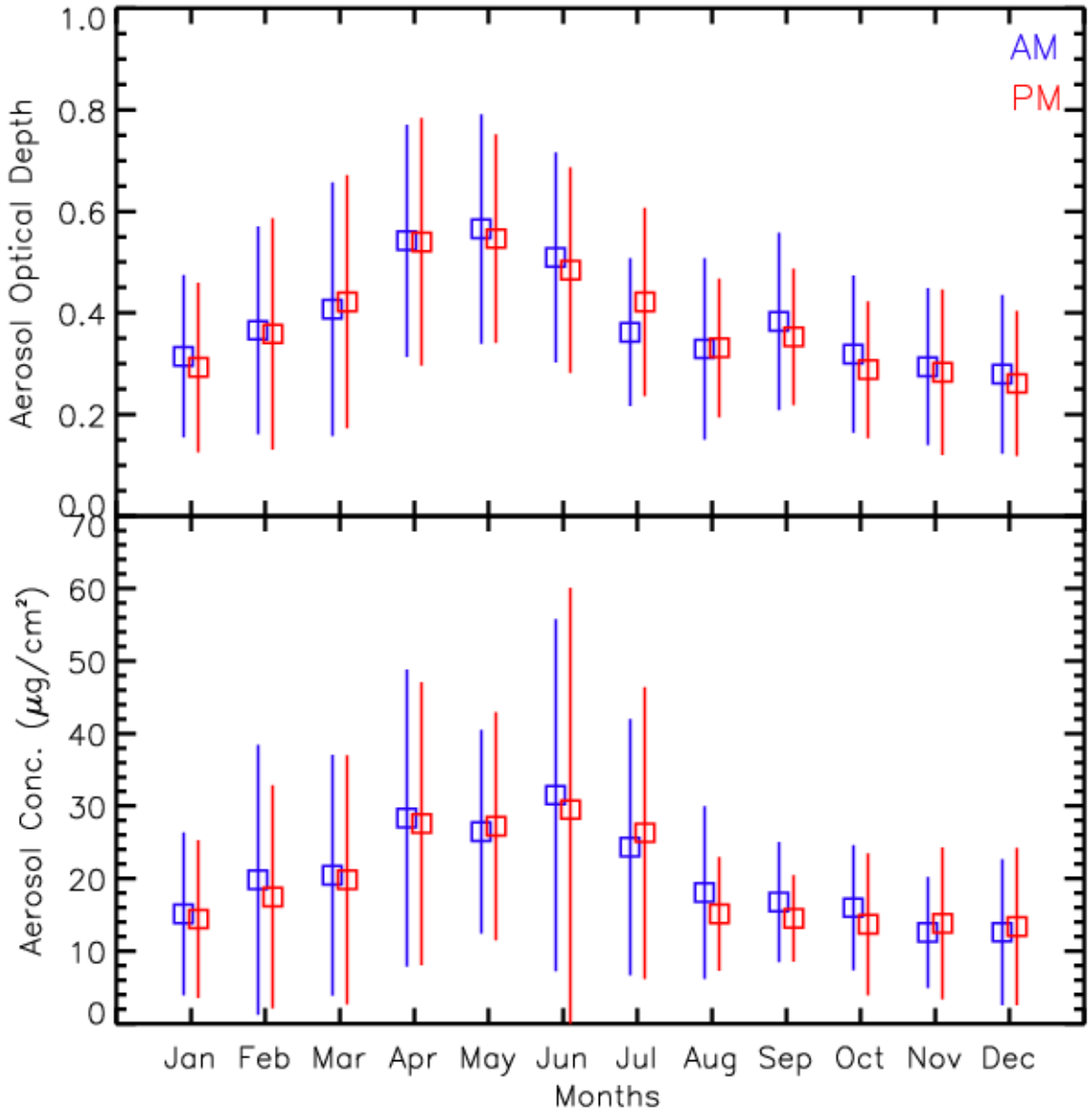

Figure 9: Column integrated MODIS monthly average AOD and mass concentration over Kathmandu based on the data from Jan 2015 - Dec 2019. The blue line illustrates the Terra (AM) data; the red line illustrates the Aqua (PM) data.

The issue arising from comparing MODIS based AOD data with direct measurements is not new. One reason for the difference in the observations is related to the fact that MODIS data are column integrated and therefore do not only represent near-surface pollution levels. Nevertheless, it is not readily evident, why in particular winter pollution levels are relatively low. It is, however, well-aligned with the findings of Filonchyk et al. (2019) for China, who observed seasonal AOD variation maxima in spring and summer and minimum in autumn and winter and explain it with hygroscopic growth of aerosols, the formation of

secondary aerosols and pollutants as a result of agricultural biomass combustion after crop harvesting. It is conceivable that this may also be a factor explaining the seasonal variation of the AOD and particulate matter data that were computed for this study. Das et al. (2020) point toward the open burning of crop residue as an important source of air pollution in Nepal and found that February to May accounted for 86.16% of the total emissions, with the peak occurring in April. This finding is generally aligned with our observation of monthly AOD data.

Jethva et al. (2019) and Sembhi et al. (2020) also confirm that the agricultural fire activity led to a significant increase in aerosol loading over the Indo-Gangetic Plain over the past decades.

We conclude that the MODIS data, while being valuable for assessing total atmospheric pollution data in the region, are not well suited to assess urban air pollution levels on a smaller scale in the Kathmandu Valley.

Filonchyck et al. (2019a) found high AOD values in China in the densely populated eastern regions with annual values over 0.6. In another study in China, Fylonchyk et al. (2019b) found annual AOD values ranging from less than 0.25 in sparsely populated areas on the Tibetan Plateau to over 0.7 in the most populous regions with the highest density of agricultural and industrial activity. In comparison, the values calculated for the broader region around Kathmandu in Nepal are considerably lower throughout most of the year except for April, May, and June; however, as stated before, they are not representative of Kathmandu itself.

3.3. CAMS and MERRA-2 Reanalysis Data

Figure 10 shows the seasonal average $PM_{2.5}$ concentrations in India and Nepal based on the CAMS reanalysis data sets. In alignment with the observations based on satellite data, the highest pollution levels are found in northern India, irrespective of the season. However, we also observed a distinct seasonal variation characterized by the highest concentrations in winter, somewhat lower concentration in the pre- and post-monsoon seasons, and the lowest concentrations in the summer monsoon season. The average wind vectors indicate a predominantly western to northwestern airflow in the region in the winter, pre-monsoon, and post-monsoon seasons. Particularly during winter, this may result in the long-range transport of pollutants from the northern Indian hotspots to the Kathmandu Valley. This notion is supported by the observation that high pollution levels in northern India extend throughout southern Nepal during this season. It leads to the conclusion that the extremely high levels in Kathmandu during the winter may be the result of local emissions as well as long-range transportation.

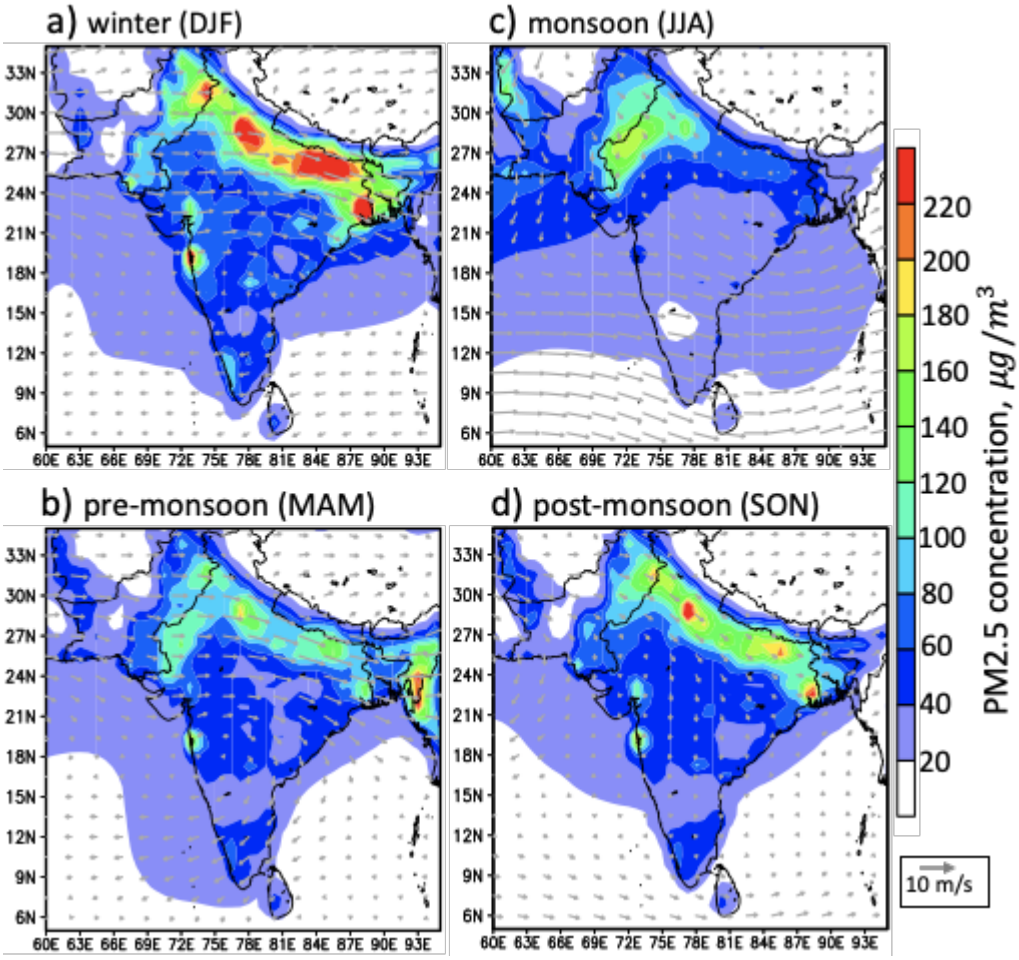

Figure 10: Seasonal average $PM_{2.5}$ concentration (color filled in µg m^{-3}) from CAMS reanalysis data wind 700 mb wind vectors; a) winter season (December-February), b) pre-monsoon season (March-May), c) summer monsoon season (June-August), and d) post-monsoon season (September-November).

Figure 11 illustrates the monthly variability of AOD based on both reanalysis datasets. Both datasets are well-aligned, showing a maximum in the pre-monsoon and a minimum in the monsoon season. This observation generally corresponds to the above-mentioned finding based on the MODIS data, the latter showing only slightly higher values throughout the year. Therefore, the explanation for the annual variability of the MODIS-based AOD data is also valid for the reanalysis-based AOD data. The interannual variability in the reanalysis datasets is relatively high in winter for the CAMS data and in spring for the MERRA-2 data. The relatively low summer AOD values are also characterized by small interannual variabilities in both datasets.

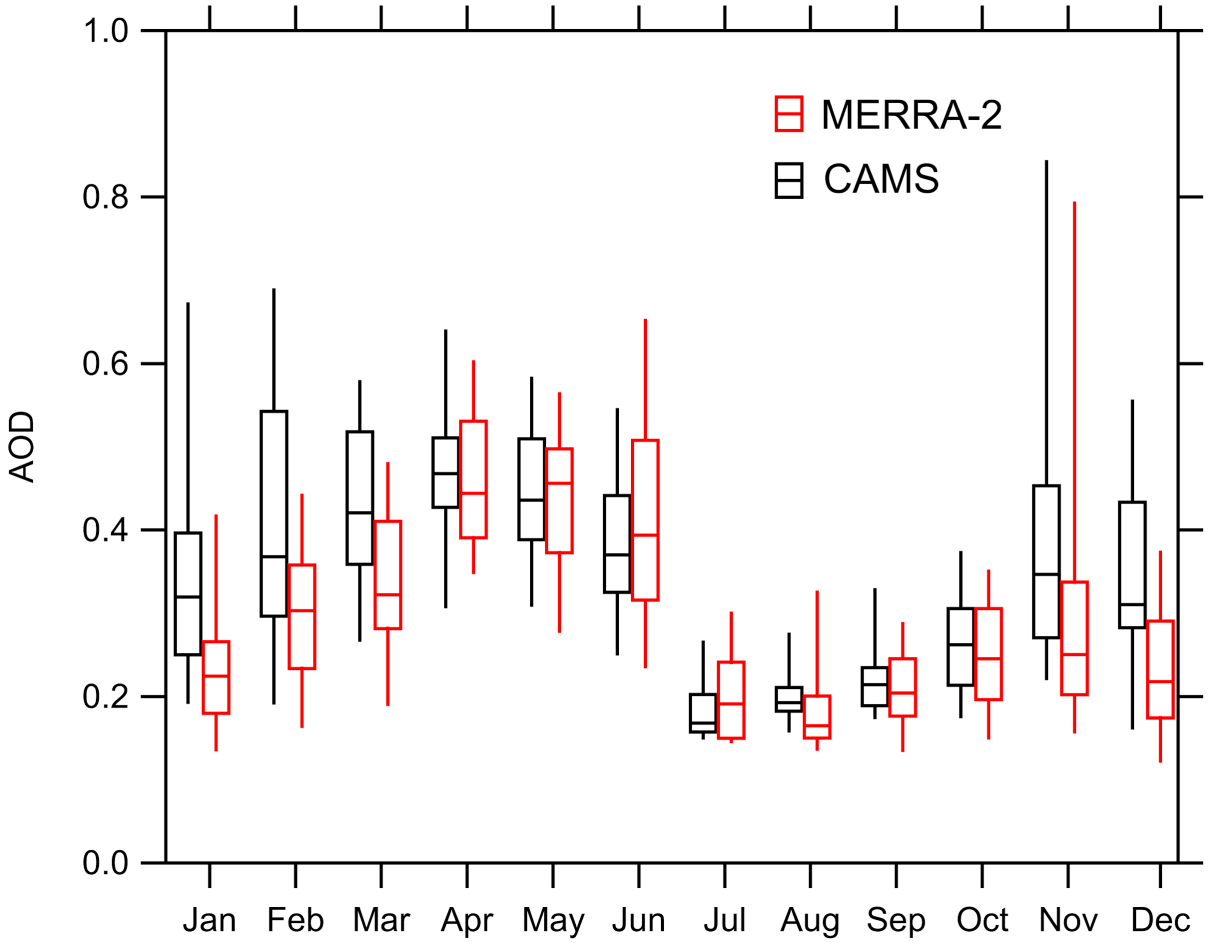

Figure 11: Box and whisker plot of the monthly average AOD distribution based on 17 years (2003-2019) of reanalysis data from CAMS (black box) and MERRA-2 (red box). The box represents the interquartile range, the horizontal line in the box is the median, and whiskers represent the 95th and 5th percentile of the data.

Monthly averages and percentiles of the $PM_{2.5}$ levels based on the reanalysis datasets are shown in Figure 12. The MERRA-2 levels are more or less a reflection of the corresponding AOD values. We observed increasing values toward the pre-monsoon season that are characterized by high interannual variabilities. The summer concentrations are consistently low with low interannual variabilities, and an increase is again noted in the post-monsoon season. This annual course has a striking resemblance with the MODIS data (Figure 9.) Similar to the MODIS data, MERRA-2 data appear to capture pollution levels at a scale that is strongly influenced by pollution levels in the larger area that are likely affected by crop residue burning rather than the smaller scale urban pollution levels in Kathmandu. In contrast, the annual cycle of the CAMS-based $PM_{2.5}$ levels shows the same characteristics as the ground-based measurement data with a distinct winter maximum and a summer

minimum. It is also noteworthy that the interannual variability of the CAMS-based $PM_{2.5}$ levels is relatively low throughout the year.

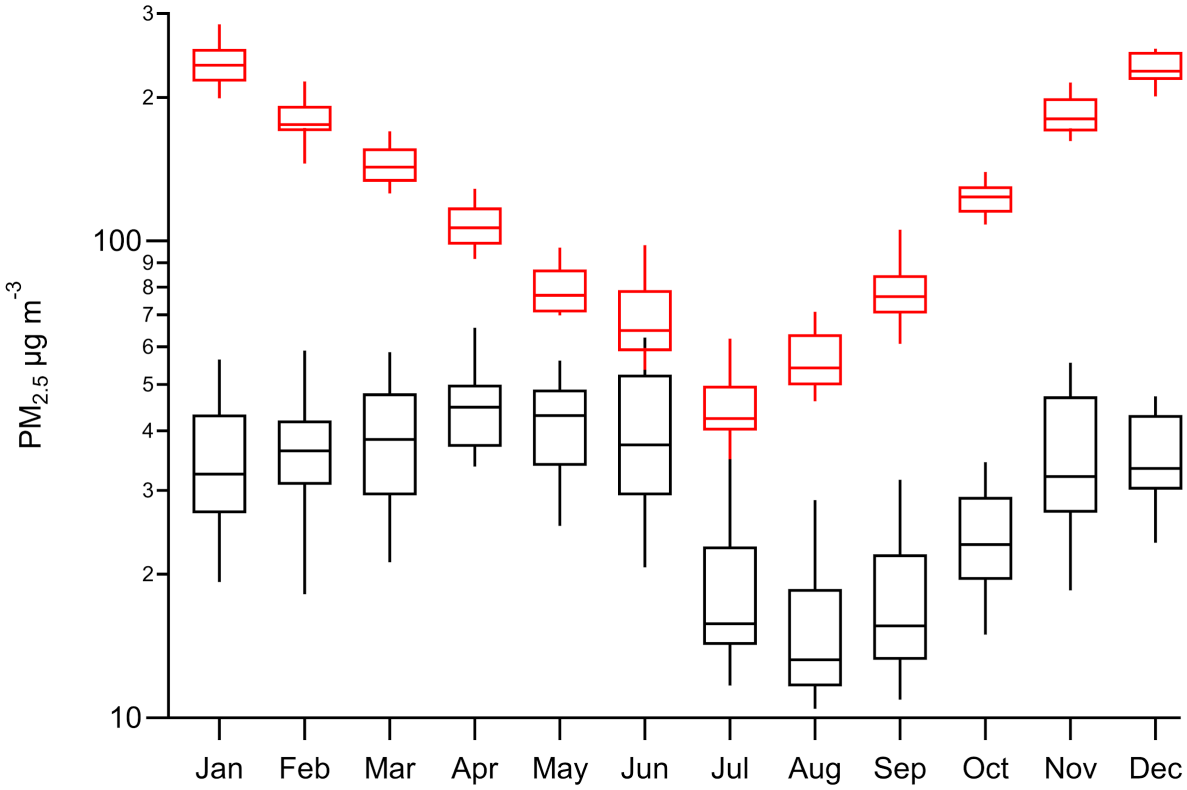

Figure 12. Box and whisker plot of the monthly average $PM_{2.5}$ concentration distribution based on 17 years (2003-2019) of reanalysis data from CAMS (red box) and MERRA-2 (black box). The box represents the interquartile range, the horizontal line in the box is the median, and the whiskers represent the 95th and 5th percentile of the data.

Diurnal cycles of pollution levels based on the CAMS reanalysis data are shown in Figure 13 for the four seasons. During all seasons, we observed an increase in pollution levels in the evening and throughout the night, which corresponds well to the findings based on the in-situ measurements. However, the secondary peak during the morning that stood out in the measurements is not reflected in the reanalysis data, which are characterized by decreasing morning values. This observation points toward the conclusion that the morning peak found only in the measurements is a local phenomenon based on the early morning traffic and the onset of industrial activities. The 0.7° x 0.7° spatial resolution of the reanalysis data is too coarse to capture this phenomenon.

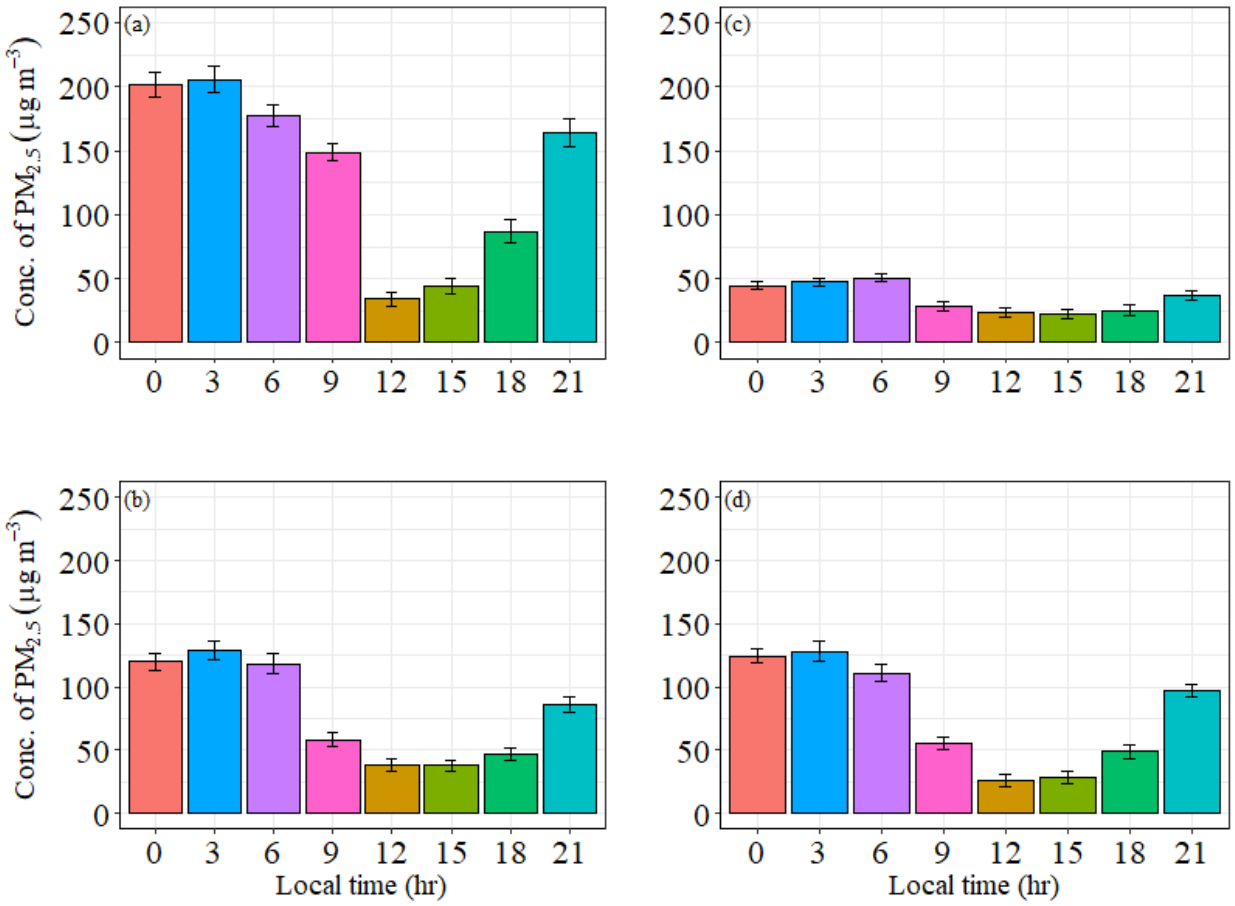

Figure 13: Diurnal variation of $PM_{2.5}$ concentration in Kathmandu, Nepal, during different seasons based on CAMS reanalysis data. a) shows the winter season (December-February), b) shows the pre-monsoon season (March-May), c) shows the summer monsoon season (June-August), and d) shows the post-monsoon season (September-November).

Figure 14 shows the seasonal and annual $PM_{2.5}$ concentration trends in the Kathmandu Valley based on CAMS reanalysis data and differentiated by season. All seasons are characterized by increasing pollution levels from 2003 to 2019, with the highest increases noted for the high-pollution winter and post-monsoon seasons. For example, we note a significant approximately 15% increase during winter from 200 to 230 $\mu g\ m^{-3}$, which constitutes an average annual increase of almost 2 $\mu g\ m^{-3}$. Even though a differentiated analysis of factors that may have contributed to this increase is not possible in the framework of the current study, it is reasonable to link it to the increase in traffic and industrial activities that occurred in the Kathmandu Valley.

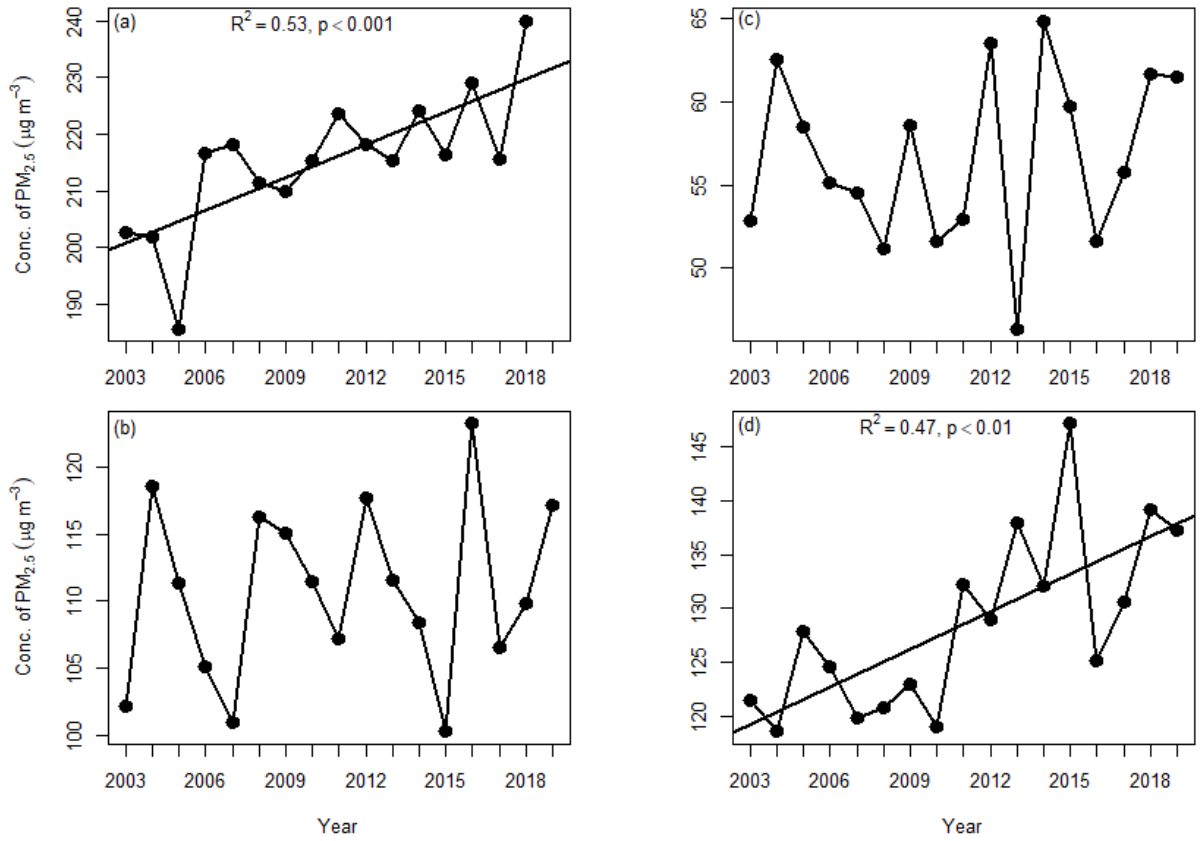

Figure 14: Seasonal and annual $PM_{2.5}$ concentration trend in Kathmandu based on reanalysis CAMS data; a) winter season (December-February), b) pre-monsoon season (March-May), c) summer monsoon season (June-August), and d) post-monsoon season (September-November). The dashed line in all panels shows the linear trend, and the p-value is shown if the trend is statistically significant.

In the following, we document our approach to reconcile reanalysis and ground-based pollution levels statistically. As evidenced by Figure 15, the CAMS and ground-based observation data are highly correlated. The correlation between MERRA-2 and ground-based observation data is relatively weak and, in addition, MERRA-2 is generally underestimating surface pollution levels in Kathmandu. This observation is in line with the findings of Navinya et al. (2020), who compared MERRA data with ground-based observations in India between 2015 and 2018.

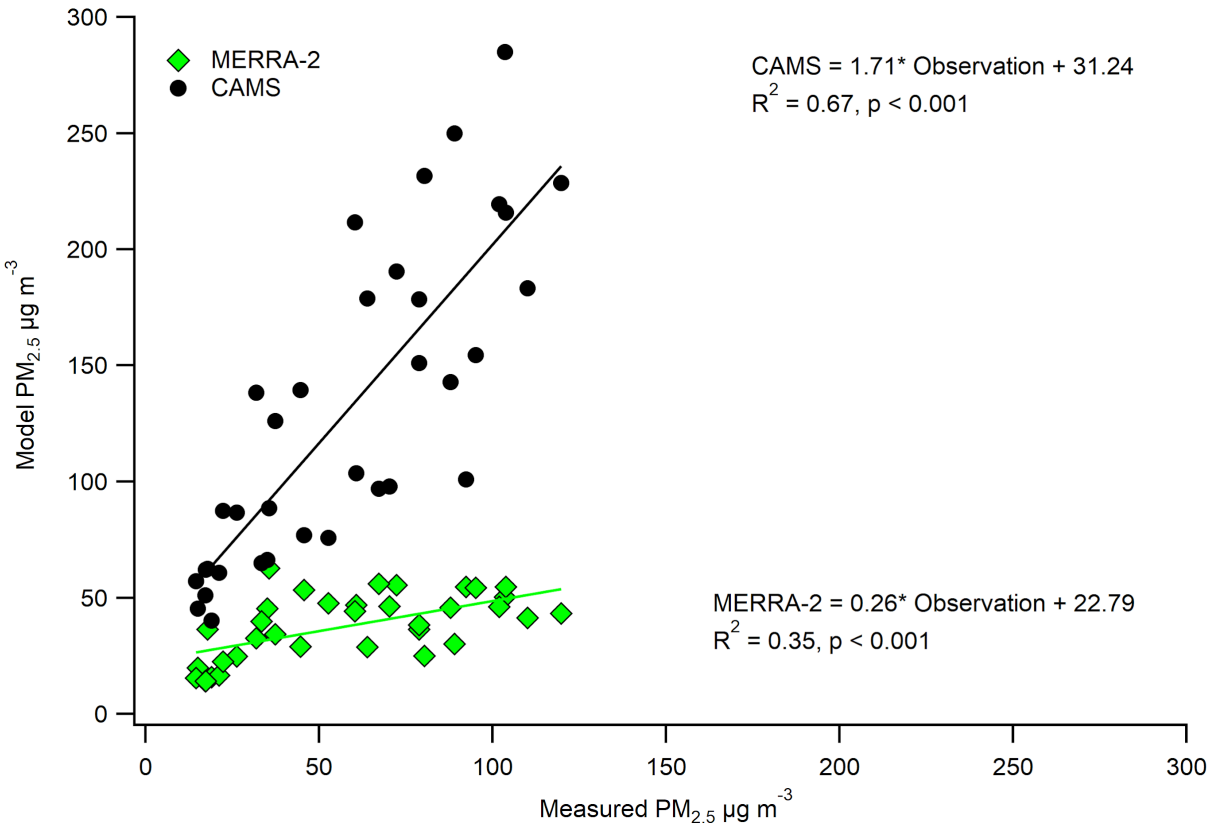

Figure 15: Comparison of CAMS and MERRA-2 $PM_{2.5}$ with the ground-based observation.

The comparison between monthly averages of direct measurements with the CAMS and MERRA-2 data is shown in Figure 16. As was to be expected from the correlation coefficients and the previous considerations regarding the annual cycles of the data, the MERRA-2 pollution levels are generally not suitable to estimate near-ground pollution levels in central Kathmandu. The only exception to this statement pertains to the summer months, during which both datasets are very closely aligned. In contrast, even though the CAMS data are overestimating near-ground pollution levels by a considerable margin, general features of the cycles between the datasets are well aligned. Both datasets correspond very well in terms of the overall annual trend of the data. The differences are most prominent during the winter season. Shortly before, during, and shortly after the summer monsoon season, the values are aligned somewhat better, even though CAMS is still overestimating the levels.

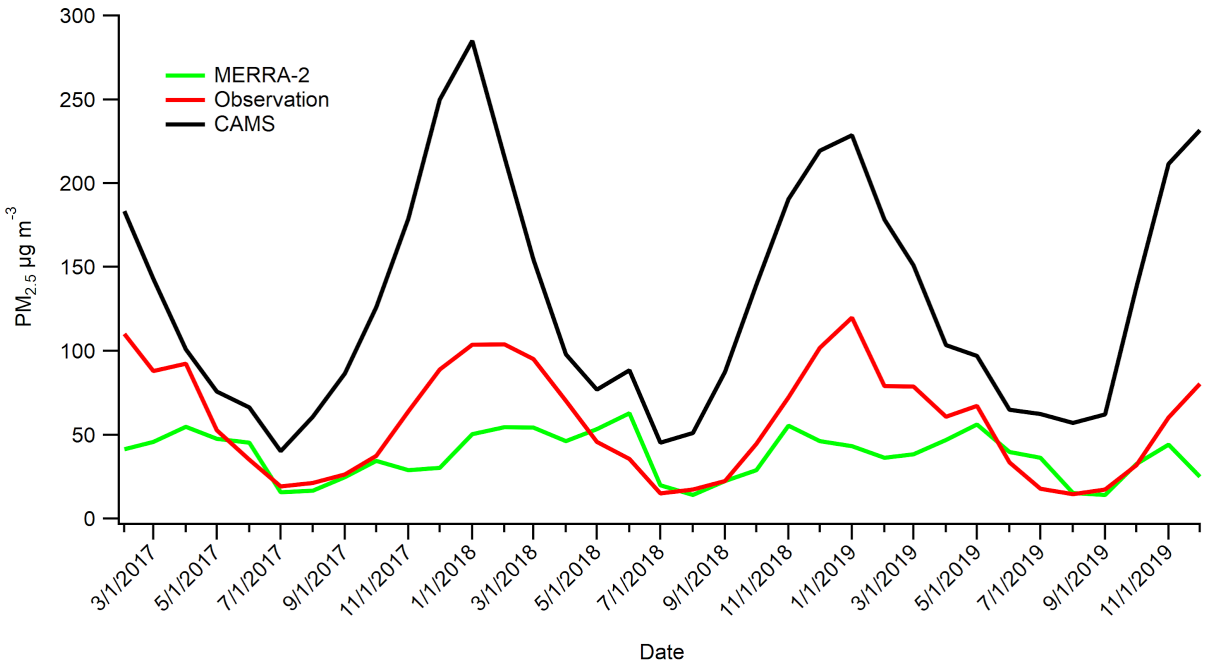

Figure 16: Monthly average $PM_{2.5}$ concentration ground-based observation, CAMS, and MERRA-2 reanalysis data.

The general alignment of seasonal fluctuations between the CAMS and near-ground observation data prompted us to make a simple adjustment of the former by using a linear function to reconcile them with the latter. The results are shown in Figure 17. It becomes obvious that, following the adjustment, CAMS data are not only well aligned with the observations in terms of general fluctuation features but also in terms of the magnitude of pollution levels. Based on a simple linear regression adjustment, it is noteworthy that the coarse-gridded CAMS reanalysis data appear to adequately capture the relatively small-scale urban pollution levels. We conclude that CAMS may be used to look at long term air pollution data in locations, especially smaller areas, where ground measurement data are not available. This observation supports the notion that the 17-year trends discussed above are indeed reflective of the near-ground pollution levels in Kathmandu itself.

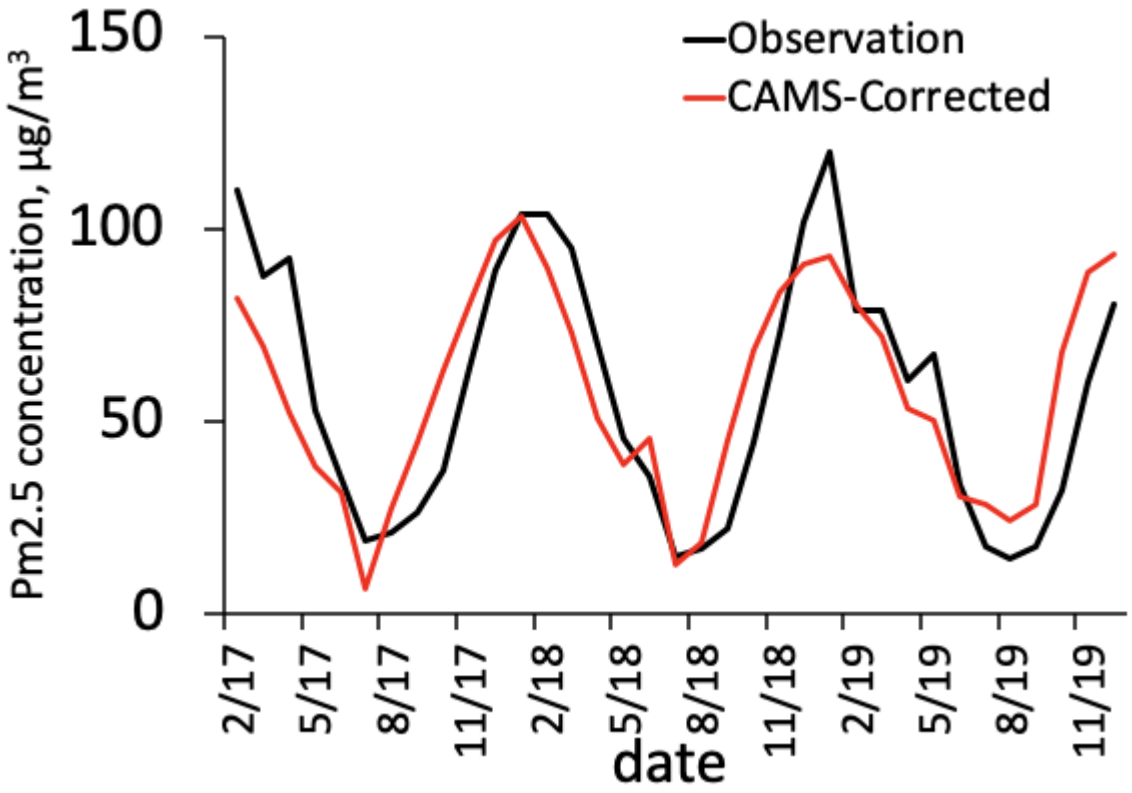

Figure 17: Monthly PM2.5 averages based on direct measurements (black line) and adjusted CAMS data (red line)

4. Discussion and Conclusion

Figure 18 illustrates the average daily $PM_{2.5}$ concentrations in Kathmandu, classified by the Air Quality Index (AQI) categories. While the percentage of days in the "very unhealthy" category is small, around 37% of the days are categorized as "unhealthy," which makes "unhealthy" the most common class for pollution levels in Kathmandu.

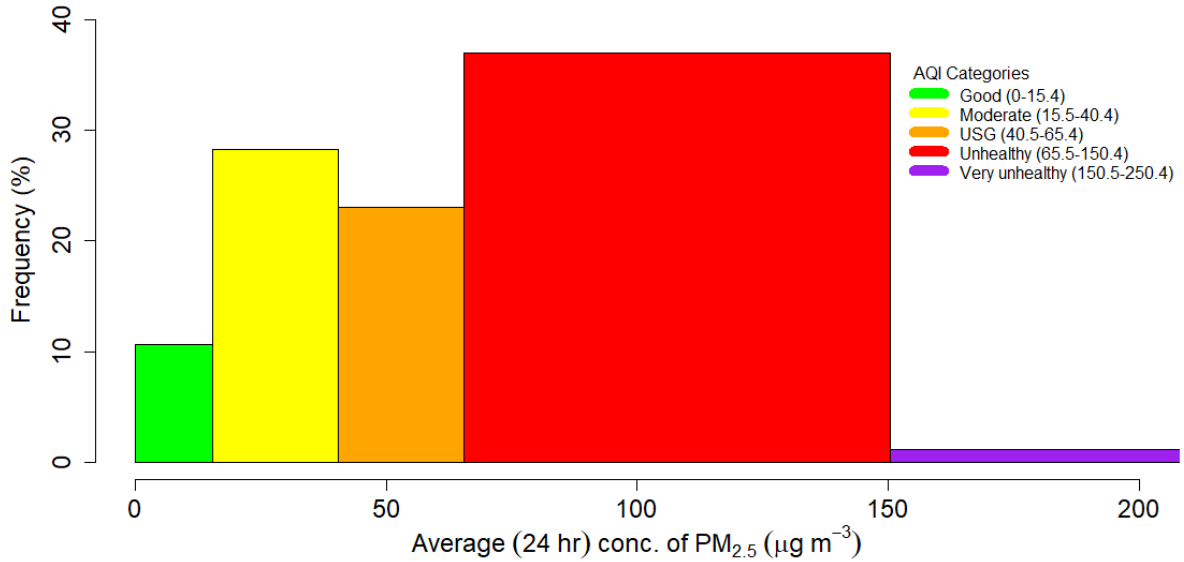

Figure 18: Average daily $PM_{2.5}$ concentrations in Kathmandu, classified by the Air Quality Index (AQI) categories.

Seasonal daily $PM_{2.5}$ concentrations in Kathmandu, classified by the Air Quality Index (AQI) categories, are shown in Figure 19. During winter, the vast majority of days (85%) are categorized as "unhealthy," and even a significant number of days (3.4%) fall into the worst category ("very unhealthy"). Only on 0.4% of all winter days can we expect good conditions, and even "moderate" pollution levels can only be expected occasionally (1.9%). In terms of particulate air pollution exposure, it certainly is considerably healthier to be outside in summer when only 0.7% of the days are labeled "unhealthy," and "very unhealthy" days do not occur. Of the two transitional seasons, the pre-monsoon season is generally more dangerous to human health in terms of particulate pollution. 45% of all days in the pre-monsoon season are labeled "unhealthy," and even "very unhealthy" conditions, while not being common, occasionally occur (1.2%). The post-monsoon season is somewhat better, with most days being "moderate" or "unhealthy for sensitive groups," while "unhealthy" days occur less frequently (16%).

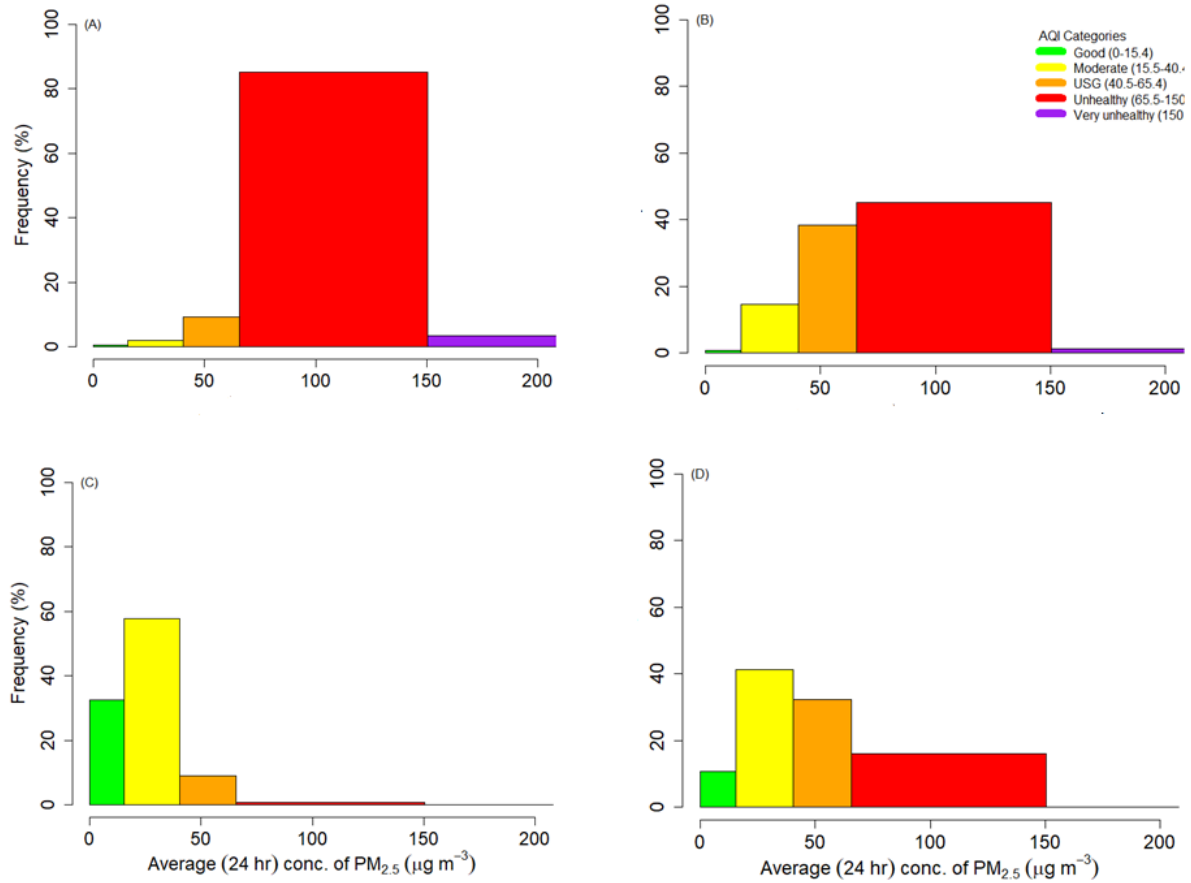

Figure 19: Seasonal daily $PM_{2.5}$ concentrations in Kathmandu, classified by the Air Quality Index (AQI) categories. (A - winter, B - pre-monsoon, C- monsoon, D- post-monsoon).

As pointed out in the introduction, air pollution is one of the greatest risks to human health in many regions of the world, including Nepal. Numerous studies (e.g., Greenstone and Fan, 2020) have demonstrated the negative impact of particulate matter on life expectancy in areas that do not meet the WHO guidelines. Chen et al. (2013) and Ebenstein et al. (2017) compared subgroups of a population that experienced prolonged exposure to different levels of particulate air pollution and were able to plausibly isolate the effect of particulate air pollution from other factors that affect health. They conclude that sustained exposure to an additional 10 µg m^{-3} of $PM_{2.5}$ reduces life expectancy by 0.98 years. Based on these studies, Greenstone and Fan (2020) infer that air pollution reduces the life expectancy of the Nepalese people by 4.7 years on average. Kathmandu is the biggest city in Nepal with an estimated 2020 population of 1.4 million people (according to www.worldpopulationreview.com), which is growing rapidly. The population of the Kathmandu Valley was about 2.5 million in 2011 census (unstats.un.org). Given these

numbers, it becomes clear that particulate matter air pollution has a devastating impact on the country and its people.

Adequate measures to address this serious problem and reduce the exorbitant pollution levels are urgently needed. To develop meaningful strategies to that end, further studies focusing on the high-resolution spatial distribution of particulate matter air pollution in the city and the Kathmandu Valley are needed.

Acknowledgments: This study utilized freely available data from different sources. We would like to acknowledge NASA's Modern-Era Retrospective Analysis, Version 2 (MERRA-2), and Moderate Resolution Imaging Spectroradiometer (MODIS), Copernicus Atmospheric Monitoring Service (CAMS), and AirNow U.S. Department of State for their efforts to make the data available for public use.

Declaration of Interest: The authors declare that they have no known competing financial interests or personal relationships that could have appeared to influence the work reported in this paper.

References

Al-Saadi, J., Szykman, J., Pierce, R.B., Kittaka, C., Neil, D., Chu, D.A., Remer, L., Gumley, L., Prins, E., Weinstock, L., MacDonald, C., Wayland, R., Dimmick, F., Fishman, J., 2005. Improving national air quality forecasts with satellite aerosol observations. Bull. Am. Meteorological Soc. 86, 1249e1261. http://dx.doi.org/10.1175/BAMS-86-9-1249.

Apte, J.S., Marshall, J.D., Cohen, A.J., Brauer, M., 2015. Addressing global mortality from ambient PM2.5. Environ. Sci. Technol. 49 (13), 8057e8066. http://dx.doi.org/10.1021/acs.est.5b01236.

Bhattarai, H., 2020. Air pollution in Kathmandu. Ecologist. https://theecologist.org/2020/mar/23/air-pollution-kathmandu

Bonasoni, P., Laj, P., Marinoni, A., Sprenger, M., Angelini, F., Arduini, J., Bonafe, U., Calzolari, F., Colombo, T., Decesari, S., Di Biagio, C., di Sarra, A. G., Evangelisti, F., Duchi, R., Facchini, M., Fuzzi, S., Gobbi, G. P., Maione, M., Panday, A., Roccato, F., Sellegri, K., Venzac, H., Verza, G., Villani, P., Vuillermoz, E. and Cristofanelli, P. (2010). Atmospheric Brown Clouds in the Himalayas: First two years of continuous observations at the Nepal Climate Observatory-Pyramid (5079 m). Atmos. Chem. Phys. 10: 7515–7531.

Buchard, V.; Randles, C. A.' da Silva, A. M.' Darmenov, A.' Colarco ,P. R.' Govindaraju, R.' Ferrare, R.' Hair, J.' Beyersdorf, A. J.' Ziemba, L. D., Yu, H. 2017. The MERRA-2 Aerosol Reanalysis, 1980 Onward. Part II: Evaluation and Case Studies, J Clim, 30(17), 6851-6872, doi:10.1175/jcli-d-16-0613.1.

Chen, Y., Ebenstein, A., Greenstone, M., & Li, H., 2013. Evidence on the impact of sustained exposure to air pollution on life expectancy from China's Huai River policy. Proceedings of the National Academy of Sciences, 110(32), 12936-12941.

Das, B., Bhave, P.V., Puppala, S.P., Shakya, K., Maharjan, B., Byanju, R.M., 2020.: A model-ready emission inventory for crop residue open burning in the context of Nepal. Environmental Pollution 266 (2020) 115069

Dhaka, S. K., Chetna, Kumar, V., Panwar, V., Dimri, A. P., Singh, N., Patra, P.K., Matsumi, Y., Takigawa, M., Nakayama, T., Yamaji, K., Kajino, M., Misra, P., Hayashida, S., 2020. PM2.5 diminution and haze events over Delhi during the COVID 19 lockdown period: an interplay between the baseline pollution and meteorology. Scientific Reports | (2020) 10:13442 | https://doi.org/10.1038/s41598-020-70179-8

Ebenstein, A., Fan, M., Greenstone, M., He, G., & Zhou, M., 2017. New evidence on the impact of sustained exposure to air pollution on life expectancy from China's Huai River Policy. Proceedings of the National Academy of Sciences, 114(39), 10384-10389.

EPA, 2012. Revised Air Quality Standards for Particle Pollution and Updates to the Air Quality Index (AQI). https://www.epa.gov/sites/production/files/2016-04/documents/2012_aqi_factsheet.pdf

EPA, 2016. NAAQS Table. https://www.epa.gov/criteria-air-pollutants/naaqs-table

EPA, 2020. Health and Environmental Effects of Particulate Matter (PM). https://www.epa.gov/pm-pollution/health-and-environmental-effects-particulate-matter-pm

Faiz, A., Ale, B. B., Nagarkoti, R. K., 2006. The role of inspection and maintenance in controlling vehicular emissions in Kathmandu Valley, Nepal, Atmos. Environ., 40, 5967–5975, 2006.

Filonchyk, M., Yan, H., Zhang, Z., 2019(a). Combined use of satellite and surface observations to study aerosol optical depth in different regions of China. Sci Rep 9, 6174. https://doi.org/10.1038/s41598-019-42466-6

Filonchyk, M., Yan, H. & Zhang, Z., 2019(b). Analysis of spatial and temporal variability of aerosol optical depth over China using MODIS combined Dark Target and Deep Blue product. Theor Appl Climatol 137, 2271–2288. https://doi.org/10.1007/s00704-018-2737-5

Flemming, J., Benedetti, A., Inness, A., Engelen, R. J., Jones, L., Huijnen, V., Remy, S., Parrington, M., 395 Suttie, M., Bozzo, A., Peuch, V.-H., Akritidis, D., and Katragkou, E., 2017. The CAMS interim Reanalysis of Carbon Monoxide, Ozone and Aerosol for 2003-2015,

682 Atmospheric Chemistry & Physics, 17, 1945–1983, https://doi.org/10.5194/acp-17-1945-
683 2017.

684 Giri, D., Murthy, K., Adhikary, P. R., and Khanal, S. N., 2006. Ambient air quality of
685 Kathmandu valley as reflected by atmospheric particulate matter concentrations (PM10),
686 Int. J. Environ. Sci. Te., 3, 403–410, 2006.

687 Greenstone, M., and Fan, C., 2020. Air Quality Life Index - Annual Update.
688 https://aqli.epic.uchicago.edu/wp-
689 content/uploads/2020/07/AQLI_2020_Report_FinalGlobal-1.pdf

690 Guo, J., Deng, M., Lee, S.S., Wang, F., Li, Z., Zhai, P., Liu, H., Lv, W., Yao, W., Li, X., 2016(a).
691 Delaying precipitation and lightning by air pollution over the Pearl River Delta. Part I:
692 observational analyses. J. Geophys. Res. Atmos. 121, 6472e6488.
693 http://dx.doi.org/10.1002/2015JD023257.

694 Guo, J.P., He, J., Liu, H.L., Miao, Y.C., Liu, H., Zhai, P.M., 2016(b). Impact of various emission
695 control schemes on air quality using WRF-Chem during APEC China 2014. Atmos. Environ.
696 140, 311e319. http://dx.doi.org/10.1016/j.atmosenv.2016.05.046.

697 Guo, J., Xia, F., Zhang, Y., Liu, H., Li, J., Lou, M., He, J., Yan, Y., Wang, F., Min, M., Zhai, P., 2017.
698 Impact of diurnal variability and meteorological factors on the PM2.5 -AOD relationship:
699 Implications for PM2.5 remote sensing. Environmental Pollution 221 (2017) 94e104

700 Gurung, A., and Bell, M.L., 2020. Exposure to airborne particulate matter in Kathmandu
701 Valley, Nepal. Journal of Exposure Science and Environmental Epidemiology (2012) 22, 235
702 -- 242

703 Hsu, A., Esty, D., Levy, M., de Sherbinin, A., 2016. The 2016 Environmental Performance
704 Index Report. New Haven, CT: Yale Center for Environmental Law and Policy.
705 http://dx.doi.org/10.13140/RG.2.2.19868.90249.

706 ICIMOD, 2007. International Center for Integrated Mountain Development, Ministry of
707 Environment, Science and Technology (MoPE), United Nations Environment Programme
708 (UNEP). Kathmandu Valley Environment Outlook. Hill Side Press, Kathmandu, 2007.

709 Inness, A., M. Ades, A. Agustí-Panareda, J. Barré, A. Benedictow, A.-M. Blechschmidt, J. J.
710 Dominguez, R. Engelen, H. Eskes, J. Flemming, V. Huijnen, L. Jones, Z. Kipling, S. Massart, M.
711 Parrington, V.-H. Peuch, M. Razinger, S. Remy, M. Schulz, and M. Suttie, 2019: The CAMS
712 reanalysis of atmospheric composition. Atmos. Chem. Phys., 19, 3515–3556.
713 https://doi.org/10.5194/acp-19-3515-2019.

714 Inness, A., Blechschmidt, A.-M., Bouarar, I., Chabrillat, S., Crepulja, M., Engelen, R. J., Eskes,
715 H., Flemming, J., Gaudel, A., Hendrick, F., Huijnen, V., Jones, L., Kapsomenakis, J., Katragkou,

716 E., Keppens, A., Langerock, B., de Mazière, M., Melas, D., Parrington, M., Peuch, V. H.,
717 Razinger, M., Richter, A., Schultz, M. G., Suttie, M., Thouret, V., Vrekoussis, M., Wagner, A.,
718 and Zerefos, C., 2015: Data assimilation of satellite retrieved ozone, carbon monoxide and
719 nitrogen dioxide with ECMWF's Composition-IFS, Atmos. Chem. Phys., 15, 5275– 5303,
720 https://doi.org/10.5194/acp-15-5275-2015.

721 IPCC, 2013. Climate change 2013: the physical science basis. In: Stocker, T.F., Qin, D.,
722 Plattner, G.-K., Tignor, M., Allen, S.K., Boschung, J., Nauels, A., Xia, Y., Bex, V., Midgley, P.M.
723 (Eds.), Contribution of Working Group I to the Fifth Assessment Report of the
724 Intergovernmental Panel on Climate Change. Cambridge University Press, Cambridge,
725 United Kingdom and New York, NY, USA, p. 1535.

726 Islam, R., Jayarathne, T., Simpson, I.J., Werden, B., Maben, J., Gilbert, A., Praveen, P. S.,
727 Adhikari, S., Panday, A. K., Rupakheti, M., Blake, D.R., Yokelson, R. J., DeCarlo, P. F., Keene, W.
728 C., E. Stone, A., 2020. Ambient air quality in the Kathmandu Valley, Nepal, during the pre-
729 monsoon: concentrations and sources of particulate matter and trace gases. Atmos. Chem.
730 Phys., 20, 2927–2951, 2020. https://doi.org/10.5194/acp-20-2927-2020.

731 Jethva, H., Torres, O., Field, R., Lyapustin, A., Gautam, R., & Kayetha, V.,2019. Connecting
732 Crop Productivity, Residue Fires, and Air Quality over Northern India. Scientific Reports. 9.
733 16594. 10.1038/s41598-019-52799-x.

734 Just, A., De Carli, M. Shtein, A., Dorman, M., Lyapustin, A. Kloog, I. (2018): Correcting
735 Measurement Error in Satellite Aerosol Optical Depth with Machine Learning for Modeling
736 PM2.5 in the Northeastern USA. Remote Sens. 2018, 10(5), 803;
737 https://doi.org/10.3390/rs10050803

738 Kaufman, Y.J., Tanre, D., Boucher, O., 2002. A satellite view of aerosols in the climate system.
739 Nature 114 (13). http://dx.doi.org/10.1038/nature01091.

740 King, M. D., Kaufman, Y. J., Menzel, W. P., Tanré, D., 1992. Remote sensing of cloud, aerosol,
741 and water vapor properties from the Moderate Resolution Imaging Spectrometer (MODIS),
742 IEEE Trans. Geosci. Remote Sensing, 30, 2–27

743 Levy, R. C., Mattoo ,S., Remer, L. A., Sayer, A. M., Patadia, F., and Hsu, N. C., 2013. The
744 Collection 6 MODIS aerosol products over land and ocean, Atmos. Measure. Tech., 6, 2989 –
745 3034, doi:10.5194/amt-6-2989-2013.

746 Li, Z., Niu, F., Fan, J., Liu, Y., Rosenfeld, D., Ding, Y., 2011. Long-term impacts of aerosols on
747 the vertical development of clouds and precipitation. Nat. Geosci. 4, 888e894.

748 Lin, C., Li, Y., Yuan, Z., Lau, A.K.H., Li, C., Fung, J.C.H., 2015. Using satellite remote sensing
749 data to estimate the high-resolution distribution of ground-level PM2.5. Remote Sens.
750 Environ. 156, 117e128. http://dx.doi.org/10.1016/j.rse.2014.09.015.

751 Mahapatra, P. S., Puppala, S. P., Adhikary, B., Shrestha, K. L., Dawadi, D. P., Paudel, S. P., and
752 Panday, A. K.: Air quality trends of the Kathmandu Valley: A satellite, observation and
753 modeling perspective, Atmos. Environ., 201, 334–347,
754 https://doi.org/10.1016/j.atmosenv.2018.12.043, 2019.

755 Marinoni, A., Cristofanelli, P., Laj, P., Duchi, R., Calzolari, F., Decesari, S., Sellegri, K.,
756 Vuillermoz, E., Verza, G., Villani, P. and Bonasoni, P. (2010). Aerosol mass and black carbon
757 concentrations, a two year record at NCO-P (5079 m, Southern Himalayas). Atmos. Chem.
758 Phys. 10: 8551–8562.

759 Mool, E., Bhave, P.V., Khanal, N., Byanju, R.M., Adhikari, S., Das, B., Puppala, S.P., 2020.
760 Traffic Condition and Emission Factor from Diesel Vehicles within the Kathmandu Valley.
761 Aerosol and Air Quality Research, 20: 395–409, 2020. ISSN: 1680-8584 print / 2071-1409
762 online. Doi: 10.4209/aaqr.2019.03.0159

763 Mues, A., Lauer, A., Lupascu, A., Rupakheti, M, Kuik, F., Lawrence, M.G., 2018. WRF and
764 WRF-Chem v3.5.1 simulations of meteorology and black carbon concentrations in the
765 Kathmandu Valley. Geosci. Model Dev., 11, 2067–2091, 2018
766 https://doi.org/10.5194/gmd-11-2067-2018

767 Navinya,C.D. , Vinoj, V., Satyendra, Pandey, K., 2020. Evaluation of PM2.5 Surface
768 Concentrations Simulated by NASA's MERRA Version 2 Aerosol Reanalysis over India and
769 its Relation to the Air Quality Index. Aerosol and Air Quality Research, 20: 1329–1339,
770 2020 ISSN: 1680-8584 print / 2071-1409 online
771 https://doi.org/10.4209/aaqr.2019.12.0615
772
773 Neupane, B.B., Sharma, A., Giri, B., Joshi, M.K., 2020. Characterization of airborne dust
774 samples collected from core areas of Kathmandu Valley. Heliyon. Vol. 6, Issue 4, April 01,
775 2020. DOI: https://doi.org/10.1016/j.heliyon.2020.e03791
776
777 Panday, A. and Prinn, R. G., 2009. Diurnal cycle of air pollution in the Kathmandu Valley,
778 Nepal: Observations, J. Geophys. Res., 114, D09305, doi:10.1029/2008JD009777, 2009.

779 Panday, A., Prinn, R. G., and Schär, C., 2009. Diurnal cycle of air pollution in the Kathmandu
780 Valley, Nepal: 2. Modeling results, J. Geophys. Res., 114, D21308,
781 doi:10.1029/2008JD009808, 2009

Putero, D., Cristofanelli, P., Marinoni, A., Adhikary, B., Duchi, R., Shrestha, S. D., Verza, G. P., Landi, T. C., Calzolari, F., Busetto, M., Agrillo, G., Biancofiore, F., Di Carlo, P., Panday, A. K., Rupakheti, M., and Bonasoni, P., 2015. Seasonal variation of ozone and black carbon observed at Paknajol, an urban site in the Kathmandu Valley, Nepal, Atmos. Chem. Phys., 15, 13957–13971, https://doi.org/10.5194/acp-15-13957-2015, 2015.

Ram, K., Sarin, M.M. and Hegde, P. (2010). Long-term record of aerosol optical properties and chemical composition from a high-altitude site (Manora Peak) in Central Himalaya. Atmos. Chem. Phys. 10: 11791–11803.

Randles, C. A., da Silva, A. M., Buchard, V., Colarco, P. R., Darmenov, A., Govindaraju, R.; Smirnov, A., Holben, B., Ferrare, R., Hair, J., Shinozuka, Y., Flynn, C. J., 2017. The MERRA-2 Aerosol Reanalysis, 1980 - onward, Part I: System Description and Data Assimilation Evaluation, J Clim, 30(17), 6823-6850, doi:10.1175/JCLI-D-16-0609.1.

Remer, L. A., Kaufman, Y. J., Tanré, D., Mattoo, S., Chu, D. A., Martins, J. V., Li, R-.R., Icholu, C., Levy, R. C., Kleidman, R. G., Eck, T. F., Vermote, E., Holben B. N., 2005. The MODIS aerosol algorithm, products and validation. J. Atmos. Sci., 62(4), 947 – 973.

Rosenfeld, D., Lohmann, U., Raga, G.B., O'Dowd, C.D., Kulmala, M., Fuzzi, S., Reissell, A., Andreae, M.O., 2008. Flood or drought: how do aerosols affect precipitation? Science 321, 1309e1313.

Sadavarte, P., Rupakheti, M., Bhave, P., Shakya, K., Lawrence, M., 2019. Nepal emission inventory – Part I: Technologies and combustion sources (NEEMI-Tech) for 2001–2016. Atmos. Chem. Phys., 19, 12953–12973, 2019. https://doi.org/10.5194/acp-19-12953-2019

Saikawa, E., Wu, Q., Zhong, M., Avramov, A., Ram, K., Stone, E. A., Stockwell, C. E., Jayarathne, T., Panday, A. K., Yokelson, R. J., 2020. Garbage Burning in South Asia: How Important Is It to Regional Air Quality? Environ. Sci. Technol. 2020, 54, 9928−9938

Sembhi, H. , M. Wooster, T. Zhang, S. Sharma, N. Singh, S. Agarwal, H.Boesch, S. Gupta, A. Misra, S. N. Tripathi, S. Mor, R. Khaiwal , 2020. Post-monsoon air quality degradation across Northern India: Assessing the impact of policy-related 2 shifts in timing and amount of crop residue burnt. Environmental Research Letters · July 2020. DOI: 10.1088/1748-9326/aba714

Schwartz, J.D., Melly, S.J., Koutrakis, P., Coull, B.A., Kloog, I., Zanobetti, A., Shi, L., 2015. Low-concentration PM2.5 and mortality: estimating acute and chronic effects in a population-based study. Environ. Health Perspect. 124 (1), 46. http://dx.doi.org/10.1289/ehp.1409111.

Shakya, K.M., M. Rupakheti, A. Shahi, R. Maskey, B. Pradhan, A. Panday, S. P. Puppala, M. Lawrence, R. E. Peltier, 2017. Near-road sampling of PM2.5, BC, and fine-particle chemical components in Kathmandu Valley, Nepal. Atmos. Chem. Phys., 17, 6503–6516, 2017. https://doi.org/10.5194/acp-17-6503-2017

Sharma, C. K., 1997. Urban air quality of Kathmandu Valley "Kingdom of Nepal", Atmos. Environ., 31, 2877–2883, 1997

Sharma, R. K., Bhattarai, B. K., Sapkota, B. K., Gewali, M. B., and Kjeldstad, B, 2012. Black carbon aerosols variation in Kathmandu valley, Nepal, Atmos. Environ., 63, 282–288, 2012.

Shrestha, S. R., Kim Oanh, N. T., Xu, Q., Rupakheti, M., and Lawrence, M. G. 2013. Analysis of the vehicle fleet in the Kathmandu Valley for estimation of environment and climate co-benefits of technology intrusions, Atmos. Environ., 81, 579–590, 2013.

Srijan Lal, S., 2018. Assessment of Ambient Particulate Air Pollution and its Attribution to Environmental Burden of Disease in Kathmandu Valley, Nepal: A Review. 4(4). EAES.000592. 2018. DOI: 10.31031/EAES.2018.04.000592Location

Tanré, D., Herman, M., Kaufman, Y., 1996. Information on aerosol size distribution contained in solar reflected spectral radiances, J. Geophys. Res-Atmos, 101, 19043 - 19060

Kanawade, V.P., Srivastava, A.K., Ram, K., Asmi, E., Vakkari, V., Soni, V.K., Varaprasad, V., Sarangi, C., 2020. What caused severe air pollution episode of November 2016 in New Delhi? Atmospheric Environment, Volume 222, 1 February 2020, 117125. https://doi.org/10.1016/j.atmosenv.2019.117125

Vidot, J., Santer, R., Ramon, D., 2007. Atmospheric particulate matter (PM) estimation from SeaWiFS imagery. Remote Sens. Environ. 111, 1e10. http://dx.doi.org/10.1016/j.rse.2007.03.009.

Wang, J., Christopher, S.A., 2003. Intercomparison between satellite-derived aerosol optical thickness and PM2.5 mass: implications for air quality studies. Geophys. Res. Lett. 30 (21) http://dx.doi.org/10.1029/2003GL018174.

Wang, L., Zhang, N., Liu, Z., Sun, Y., Ji, D., Wang, Y., 2014. The influence of climate factors, meteorological conditions, and boundary-layer structure on severe haze pollution in the Beijing-Tianjin-Hebei region during January 2013. Adv. Meteorology 2014, 1e14. http://dx.doi.org/10.1155/2014/685971.

Wang, Z., Chen, L., Tao, J., Zhang, Y., Su, L., 2010. Satellite-based estimation of regional particulate matter (PM) in Beijing using vertical-and-RH correcting method. Remote Sens. Environ. 114, 50e63. http://dx.doi.org/10.1016/j.rse.2009.08.009.

Zhong, M., Saikawa, E., Avramov, A., Chen, C., Sun, B., Ye, W.; Keene, W. C., Yokelson, R. J., Jayarathne, T., Stone, E. A., Rupakheti, M., Panday, A. K., 2019. Nepal Ambient Monitoring and Source Testing Experiment (NAMaSTE): Emissions of Particulate Matter and Sulfur Dioxide from Vehicles and Brick Kilns and Their Impacts on Air Quality in the Kathmandu Valley. Atmos. Chem. Phys. 2019, 19 (12), 8209–8228.